International Journal of Food Microbiology 383 (2022) 109962

Contents lists available at ScienceDirect

International Journal of Food Microbiology

journal homepage: www.elsevier.com/locate/ijfoodmicro

Deciphering the virulence potential of *Listeria monocytogenes* in the Norwegian meat and salmon processing industry by combining whole genome sequencing and *in vitro* data

Eva Wagner [a,*,1], Annette Fagerlund [a], Sarah Thalguter [b,c], Merete Rusås Jensen [a], Even Heir [a], Trond Møretrø [a], Birgitte Moen [a], Solveig Langsrud [a], Kathrin Rychli [b]

[a] Nofima - Norwegian Institute of Food, Fisheries and Aquaculture Research, Ås, Norway
[b] Unit of Food Microbiology, Institute of Food Safety, Food Technology and Veterinary Public Health, University of Veterinary Medicine, Vienna, Austria
[c] FFoQSI GmbH – Austrian Competence Centre for Feed and Food Quality, Safety and Innovation, Tulln, Austria

ARTICLE INFO

Keywords:
Foodborne infection
Listeriosis
Next generation sequencing
Food processing environment
In vitro virulence
Pathogenicity
inlA

ABSTRACT

Whole genome sequencing (WGS) of foodborne pathogens such as *Listeria monocytogenes* is globally on the rise in the food industry. It provides an improvement for proactive surveillance and source-tracking and allows in-depth genetic characterization of the pathogen. In the present study, the virulence gene profile including 99 virulence genes of 767 *L. monocytogenes* isolates from the Norwegian meat and salmon processing industry was characterized. The isolate collection comprised 28 clonal complexes (CCs) that occur globally. We additionally determined the *in vitro* virulence potential for 13 major CCs in human intestinal epithelial Caco2 cells using cocktails of three to six representative isolates. Our aim was to test whether the virulence potential could be predicted from the virulence gene profiles to estimate the application potential of WGS in risk assessment in the food industry.

The virulence gene profiles were highly conserved within the individual CCs and similar among phylogenetically closely related CCs. We observed a CC-associated distribution of accessory virulence genes in addition to different length polymorphisms. Furthermore, we detected different premature stop codons (PMSC) in the *inlA* gene, which were mainly present in CC9, CC121 and CC5 isolates. Accordingly, CC9 and CC5 were unable to invade Caco2 cells, whereas CC121 showed moderate virulence potential due to the presence of an isolate harboring full-length *inlA*. The highest invasion was observed for CC403 and CC415, potentially due to the presence of accessory virulence genes. We demonstrated that CC14, which harbored full-length *inlA*, was unable to invade Caco2 cells due to a low *inlA* gene expression. Reconstruction of *inlA* in CC9 and CC121 isolates showed that without the presence of InlA on the cell wall (as detected in the CC9 isolates), invasion into host cells failed.

Our study showed that predicting the virulence potential based on genetic virulence profiles provides valuable information for risk assessment in the food industry but also has its limitations. The mere presence of a full-length *inlA* gene is not sufficient for virulence, but gene expression and the presence of the protein on the cell wall is required for the successful invasion of *L. monocytogenes* into host cells. Moreover, hypovirulent CCs like CC121 were among the most abundant human clinical isolates in Norway despite harboring a PMSC mutation in the *inlA* gene. In conclusion, our study highlights that combining genotypic and phenotypic data is of great importance to improve the informative value of applying WGS in the food industry.

1. Introduction

Listeriosis is a rare, yet reoccurring, disease associated with high rates of both morbidity and mortality in vulnerable patient groups, such as elderly and/or immunocompromised individuals as well as pregnant individuals and their unborn or newborn babies. Symptoms range from a self-limiting febrile gastroenteritis to septicemia and subsequent infection of the central nervous system or crossing of the blood-placenta

* Corresponding author at: Institute of Food Science, University of Natural Resources and Life Sciences, Muthgasse 18, 1190 Vienna, Austria.
E-mail address: wagner.eva@boku.ac.at (E. Wagner).
[1] Present address: Institute of Food Science, University of Natural Resources and Life Sciences, Vienna, Austria.

https://doi.org/10.1016/j.ijfoodmicro.2022.109962
Received 13 July 2022; Received in revised form 28 September 2022; Accepted 29 September 2022
Available online 8 October 2022

barrier resulting in stillbirth or neonatal infection (Schlech, 2019). The causative foodborne pathogen *Listeria monocytogenes* is therefore of significant global concern. Listeriosis is linked to consumption of contaminated ready-to-eat food products like lightly processed fish products, meat products and soft cheeses (EFSA BIOHAZ et al., 2018). *L. monocytogenes* has continuously been reported to be present in the processing environment of meat and fish products in many countries (Félix et al., 2022), including Norway (Møretrø et al., 2017), and the food industry is using considerable resources to monitor and control *L. monocytogenes* as well as for costs linked to recalls and outbreaks. *L. monocytogenes* is ubiquitously present in the environment and adapted to many stress conditions including wide ranges of pH and temperature, high salt concentrations, low nutrient availability and low water activity. The remarkable adaptation of this pathogen to conditions in the food processing environment, including cleaning and disinfection processes and food conservation procedures, favors contamination of food products (Bucur et al., 2018; Jordan et al., 2018).

L. monocytogenes is a genetically heterogeneous species divided into four phylogenetic lineages, of which lineage I and II are the most prevalent, and >100 clonal complexes (CCs) based on multilocus sequence typing (MLST) and whole-genome phylogenetic analysis. There is evidence for a high variability of prevalence, pathogenicity and stress response of different CCs. Isolates of CC121, CC8, CC1, CC9, CC37, CC7, CC6 and CC2 are globally among the most frequently isolated clonal complexes with geographical differences (Félix et al., 2022; Maury et al., 2016; Painset et al., 2019). Additionally, the distribution of CCs between clinical and food isolates is uneven, reflecting the pathogenic heterogeneity of *L. monocytogenes*. In order to describe this heterogeneity, the term "hypervirulence" is used for CCs that are associated with high human clinical listeriosis frequencies, while the term "hypovirulence" is used for CCs that are associated with food, food processing environments, persistence and low human clinical listeriosis frequencies. Isolates of CC1, CC2, CC4 and CC6 (all belonging to lineage I) are strongly associated with a clinical origin (defined as hypervirulent), whereas CC9 and CC121 isolates (both belonging to lineage II) are predominantly isolated from food and food processing environments (defined as hypovirulent) (Bergholz et al., 2018; Lee et al., 2018; Maury et al., 2016; Painset et al., 2019). Despite the strong evidence of heterogeneous pathogenicity of *L. monocytogenes*, all isolates are considered to display the same risk and relevance as a foodborne pathogen by food safety and regulatory authorities. Whole genome sequencing (WGS) has successfully contributed to the investigation of outbreaks and increased our understanding of genetic virulence and resistance markers in *L. monocytogenes*. Genome analyses have confirmed the diversity of virulence factors and the presence of accessory virulence genes. The use of WGS may therefore enable fine-tuning of *L. monocytogenes* risk assessment in the food industry based on genetic markers of hyper- and hypovirulence, which could allow a more targeted assessment of public health risks (EFSA et al., 2019; Njage et al., 2020).

One of the core virulence elements of *L. monocytogenes* is the *Listeria* Pathogenicity Island (LIPI)-1, which carries the master regulator of virulence genes *prfA*, and a cluster of virulence genes involved in vacuolar escape (*hly* and *plcA*), actin based motility (*actA*) and cell-cell spread (*mpl* and *plcB*) (Vázquez-Boland et al., 2001). The uptake of *L. monocytogenes* into human host cells is mainly mediated by the prominent virulence factors, Internalin A (InlA) and InlB *via* receptor-mediated endocytosis. InlA binds E-cadherin, which is present on epithelial cells, whereas InlB binds the hepatocytic growth factor receptor c-Met, present on hepatocytes, epithelial cells and other cell types (Gaillard et al., 1991; Ireton et al., 2021). Hypovirulent CCs often harbor premature stop codons (PMSCs) in the *inlA* gene, resulting in a truncated protein which lacks the C-terminal cell wall anchoring domain (Gelbíčová et al., 2015; Moura et al., 2016; Nightingale et al., 2008; Van Stelten et al., 2010). Without the exposure of InlA on the surface of *L. monocytogenes*, the invasion ability into host cells is significantly impaired (Ciolacu et al., 2014; Nightingale et al., 2005; Rousseaux et al., 2004; Rychli et al., 2017). Truncated InlA is therefore largely responsible for the hypovirulent phenotype and might be the explanation for the low presence of these CCs in human clinical listeriosis cases (Maury et al., 2016; Nightingale et al., 2005, 2008; Van Stelten et al., 2010). However, there are also additional factors mediating InlA-independent translocation across intestinal epithelial cells, such as the *Listeria* adhesion protein (LAP) (Drolia et al., 2018).

Beside the major virulence factors, other pathogenicity islands that enhance invasion, such as LIPI-3, a Listeriolysin S (LLS) biosynthetic cluster of eight genes, and LIPI-4, encoding a cellobiose-family phosphotransferase system, are accessory virulence elements found only in a subset of hypervirulent CCs (Cotter et al., 2008; Maury et al., 2016; Meza-Torres et al., 2021). Moreover, *L. monocytogenes* harbors an arsenal of virulence factors involved in the different infection stages including crossing of the intestinal barrier (like LLS, which modulates the gut microbiota) (Quereda et al., 2017), systemic dissemination, modulation of host defense mechanisms (like the *Listeria* nuclear targeted protein (LntA) (Lebreton et al., 2011).

In this study, we analyzed the diversity of 99 virulence genes in 767 *L. monocytogenes* isolates, which were collected from Norwegian meat and salmon processing factories and assigned to 28 CCs, using WGS data. Furthermore, we compared their virulence profile to that of 111 publicly available Norwegian human clinical *L. monocytogenes* isolates collected between 2010 and 2015. For 13 major CCs, we determined the virulence potential by characterizing the *in vitro* invasion into human intestinal epithelial Caco2 cells. Our aim was to test whether the virulence potential could be predicted from specific virulence gene profiles to estimate the application potential of WGS in risk assessment in the food industry. Additionally, the virulence of CC14 strains, whose virulence potential could not be explained by the virulence gene profile, and the effect of a reconstructed full-length InlA on the virulence of CC9 and CC121 isolates was characterized.

2. Materials and methods

2.1. Bacterial isolates, WGS data and phylogenetic analysis

767 *L. monocytogenes* isolates from the meat and salmon processing industry in Norway sampled between 1990 and 2020, as previously described (Fagerlund et al., 2022b) were included in this study (Table 1, Table S1). The majority of the isolates were derived from nine meat and six salmon processing factories. Six isolates were collected from other meat ($n = 5$) and salmon ($n = 1$) processing factories, respectively, in scope of previous projects (Fagerlund et al., 2016a; Fagerlund et al., 2020). WGS data analysis for all 767 isolates was performed as previously reported (Fagerlund et al., 2022b), including (i) *de novo* assembly and quality assessment of the assemblies, (ii) classification of isolates based on MLST typing into sequence types (STs) and CCs (Ragon et al., 2008), (iii) whole-genome MLST (wgMLST) analysis based on 4797 coding loci implemented in BioNumerics 7.6 (BioMérieux, https://www.bionumerics.com/news/listeria-monocytogenes-whole-genome-sequence-typing). The *L. monocytogenes* reference EGDe (GenBank accession NC_003210) was subjected to wgMLST in the current study.

Minimum spanning trees were constructed using BioNumerics based on the categorical differences in the allelic wgMLST profiles for each isolate. Loci with no allele calls were excluded in the pairwise comparison between two genomes. Calculation of pairwise wgMLST distances for the construction of Neighbor-Joining (NJ) trees was performed using the daisy function (Kaufman and Rousseeuw, 1990) from the cluster package v2.1.1 (Maechler et al., 2021) in R v4.0.4 and selection of the Gower metric. NJ trees were generated using BIONJ, an improved version of the NJ algorithm implemented in the ape package v5.4-1 in R as function bionjs (Gascuel, 1997; Paradis and Schliep, 2019; "R Core Team (2020). — European Environment Agency," n.d.). Interactive Tree Of Life (iTOL) v6.5.2 was used for visualization (Letunic and Bork, 2021). Midpoint-rooted NJ trees were presented.

Table 1
L. monocytogenes isolates.

CC	Number of isolates	STs	Lineage	Processing factory[a]	Virulence assay	
					Number of strains	STs
CC9	289	ST9 ($n = 288$), ST2344 ($n = 1$)	II	M1, M3, M4, M5, M7, M8, M9, other	4	ST9 (n = 4)
CC121	86	ST121	II	M1, M3, M4, M6, M7, M8, S2, S4, S5, S6	5	ST121 ($n = 5$)
CC7	67	ST7 ($n = 54$), ST732 ($n = 13$)	II	M2, M3, M4, M6, M7, S1, S2, other	6	ST7 (n = 5), ST732 (n = 1)
CC19	55	ST19 (n = 28), ST1416 ($n = 27$)	II	M1, M4, M6, S6	4	ST19 (n = 3), ST1416 (n = 1)
CC1	34	ST1	I	M3, S2, S6, other	3	ST1 (n = 3)
CC415	30	ST394	II	M1, M2, M4, M9, S6	3	ST394 (n = 3)
CC403	27	ST403	II	S6	3	ST403 (n = 3)
CC3	24	ST3	I	S6, other	3	ST3 (n = 3)
CC177	22	ST177	II	S1, S5, other		
CC14	20	ST14	II	M1, S1, S2, S3	3	ST14 (n = 3)
CC8	19	ST8 ($n = 18$), ST551 (n = 1)	II	M1, M2, M6, M7, S1, S2, S6	6	ST8 (n = 6)
CC37	14	ST37	II	M1, S6		
CC91	14	ST91 (n = 13), ST1607 (n = 1)	II	M1, M9, S1		
CC5	13	ST5	I	M6	3	ST5 (n = 3)
CC315	10	ST249	I	S6	3	ST249 (n = 3)
CC11	9	ST451	II	M1, M4, M8, M9, S2		
CC2	7	ST2	I	S6	3	ST2 (n = 3)
CC18	5	ST18	II	M1, M7, S6		
CC20	4	ST20	II	S2, S4, other		
CC6	3	ST6	I	M4, M9		
CC31	3	ST31	II	S2, S4, S6		
CC199	3	ST199	II	M8		
CC88	2	ST296	I	S2, S6		
CC220	2	ST220	I	M1, M9		
CC21	2	ST21	II	M3, M9		
CC4	1	ST4	I	M4		
CC101	1	ST101	II	M4		
CC200	1	ST200	II	M3		

[a] M: meat processing factory, S: salmon processing factory.

2.2. Virulence gene analysis

A BLAST search for 99 virulence-associated genes (Table S2) was performed using a local nucleotide BLAST database created for the 767 *L. monocytogenes* genomes and EGDe. Only the best hit for each query sequence in each genome was kept. In case the minimum nucleotide identity was <99 % or the length ratio of the query sequence relative to the match in the genome was different than 1, the alignments and contigs were manually inspected. In addition, the protein sequences of the BLAST hits were aligned to the query protein sequences. If the protein identity was >92 %, the gene was considered to be present. The length differences of the nucleotide and protein sequences relative to the query were analyzed (referred to length polymorphisms; Table S3 including only proteins with different lengths). The internalin genes were screened for the presence of PMSC mutations and the *inlA* PMSC were assigned to mutation types (Gelbíčová et al., 2015; Moura et al., 2016). The translated *iap* gene sequences were screened for the number of threonine and asparagine (TN) () repeats. In all genomes with a BLAST hit for *inlP1* and *inlP3*, the hypervariable genetic hotspot between the genes homologous to *lmo2025* and *lmo2026* was manually inspected to analyze the whole gene insertion (Harter et al., 2019). Structural domains of protein variants were determined using the MotifFinder tool available on the GenomeNet website of the Kyoto University Bioinformatics Center (https://www.genome.jp/tools/motif/).

2.3. Generation of inlA reconstruction mutants

InlA reconstruction mutants were generated for isolate MF4997 (CC9, *inlA* PMSC mutation type 11), MF6316 (CC9, *inlA* PMSC mutation type 12) and MF7707 (CC121, *inlA* PMSC mutation type 6) by combining two protocols (Arnaud et al., 2004; Janes and Stibitz, 2006) as previously described for *Bacillus cereus* (Fagerlund et al., 2016b). Replacement *inlA* alleles (Fig. S1) were synthesized (GenScript) and inserted into pMAD-I-*Sce*I plasmid, generating pMAD-ST9fix and pMAD-MF7077fix.

Throughout the protocol, Brain Heart Infusion (BHI) was used as a liquid medium and Tryptic Soy Agar (TSA) was used as a solid medium with and without 5 μg/ml erythromycin (for pMAD selection) and 10 μg/ml tetracycline (for pBKJ223 selection) and 50 μl/mg X-gal. DNA was isolated by resuspending single colonies in 50 μl 1× Tris-EDTA buffer and boiling them in a thermoblock for 10 min at 99 °C. The supernatants were collected after centrifugation and PCR was performed using Platinum Taq DNA polymerase (Thermo Scientific) at the following conditions: 2 min 94 °C; 30 cycles of 30s 94 °C, 30s 50 °C, 3 min 72 °C; 7 min 72 °C; hold 4 °C.

Recombinants harboring the allelic replacement pMAD constructs integrated by homologous recombination (single crossover) were electroporated with pBKJ223 in order to obtain the desired gene replacements (double crossover). Single crossover and gene replacement were confirmed by PCR (Table S4) and the *inlA* sequences of the reconstruction mutants by Sanger amplicon sequencing. The mutant strains were named MF8207 (MF4997 with reconstructed *inlA*), MF8210 (MF6316 with reconstructed *inlA*) and MF8213 (MF7707 with reconstructed *inlA*). WGS of the *inlA* reconstructed strains was performed in order to exclude additional changes in the genome. Genomic DNA was isolated using the DNeasy Blood and Tissue Kit (Qiagen). Libraries were prepared using the Nextera DNA Flex Library prep kit (Illumina) and sequenced on an Illumina MiSeq platform with 300-bp paired-end reads. Raw reads were filtered on q15, trimmed of adaptors, and read mapping-based SNP analysis was performed using the CFSAN SNP pipeline v2.1.1 (Davis et al., 2015) and default filtering settings and the respective wildtype isolate as reference genome.

2.4. Selection of isolates for in vitro virulence assays

Among the 28 different CCs, a subset of 13 CCs was selected for the determination of the invasion efficiency in human intestinal epithelial Caco2 cells (Table 1, Fig. S2). The selection of CCs was based on the prevalence in the Norwegian meat and salmon processing chain and the diversity in the virulence gene profiles (Table 1, Fig. 1). CCs of lineage I

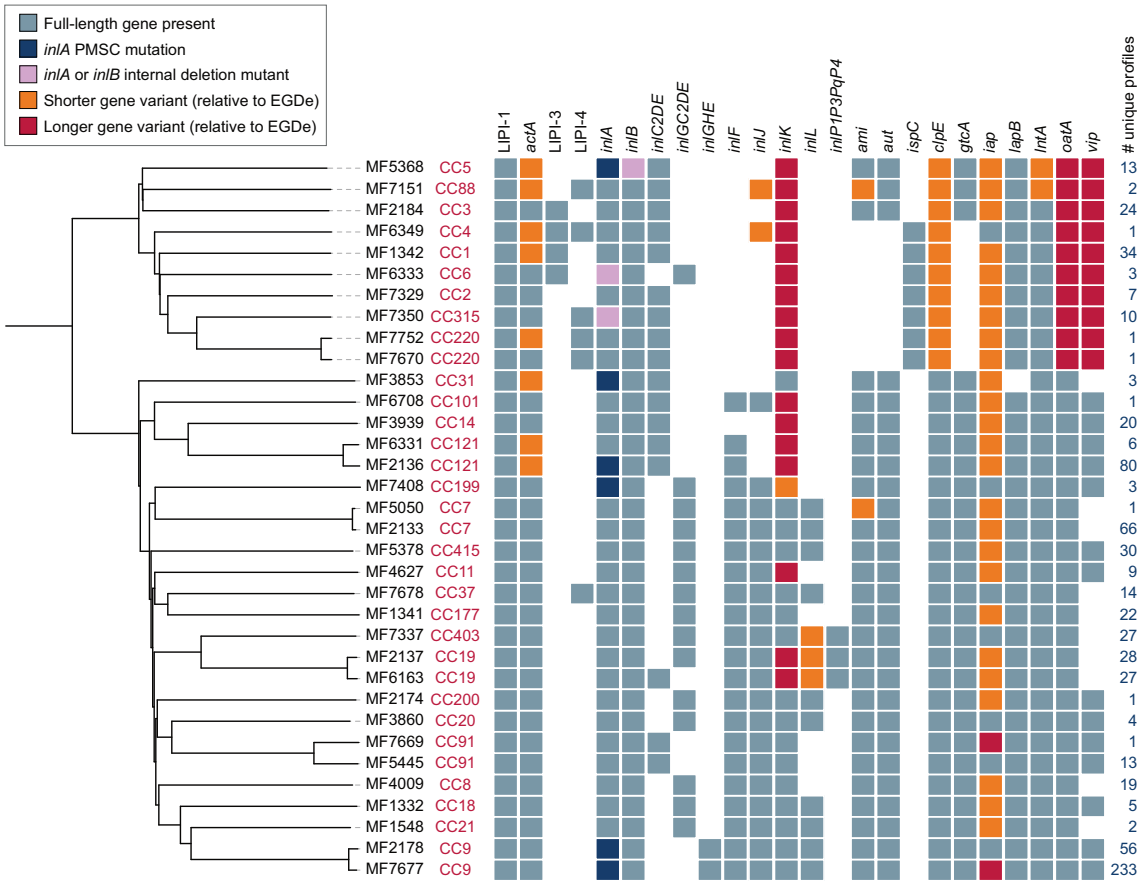

Fig. 1. Virulence gene diversity of 767 *L. monocytogenes* isolates assigned to 28 CCs. The virulence profile of one representative isolate is shown if isolates of the same CC harbor identical variants. The number of isolates represented by each profile is listed in the last column. The phylogeny is a midpoint-rooted Neighbor-Joining tree based on wgMLST analysis.

with more than five representative isolates and CCs of lineage II with >25 representative isolates were included. The 13 selected CCs were composed of five CCs from lineage I (CC1, CC2, CC3, CC5, and CC315) and eight CCs from lineage II (CC7, CC8, CC9, CC14, CC19, CC121, CC403, and CC415). Cocktails for each CC composed of three to six isolates were used for the *in vitro* virulence assays. The number and selection of isolates of each CC was based on the genetic diversity (Fig. S2), the source (Table S1) and the virulence gene profile (Fig. S3).

To study the virulence potential of CC14 isolates in more detail, MF3999 (CC14) isolated from salmon processing factory S2 was included in addition to MF7668 (CC14), one of the representative isolates in the cocktail sampled from meat processing factory M1. The number of wgMLST allelic differences between these two isolates was 72. *L. monocytogenes* EGDe was included as a reference in all virulence assays.

2.5. In vitro virulence assays

Human intestinal epithelial Caco2 cells (ATCC HTB-37), human HEPG2 hepatocytes (ATCC HB-8065) and human macrophage-like THP-1 cells (ATCC TIB-202) were used for the *in vitro* virulence assays (gentamicin protection assays). The assays were performed as previously described (Wagner et al., 2020) with some modifications. Eagle's minimum essential medium (MEM; Thermo Scientific) was used for Caco2 and HEPG2 cells and RPMI-1640 for THP1 cells throughout the assays.

Single colonies of *L. monocytogenes* were inoculated in 200 µl BHI supplemented with 5 g/l yeast extract (BHI-Y) in 96-well plates (for the assays using cocktails of three to six isolates) or 5 ml BHI-Y (for the assays using single isolates). In order to mimic reasonably realistic conditions of *L. monocytogenes* infection, two different cultivation conditions for the bacterial cultures were applied, one for the infection of Caco2 and one for HEPG2/THP1 cells. Bacteria were cultivated for 8 h at 37 °C and subsequently for 16 h at 10 °C to mimic food storage conditions prior to *L. monocytogenes* infection of Caco2 cells. OD_{600} was measured and adjusted to 0.05 in 200 µl BHI-Y for the assays using cocktails of three to six isolates from the same CC or to OD_{600} 0.1 in 5 ml BHI-Y for single isolates, and incubated for 2 h at 37 °C. This was done as the intestinal epithelium is the first entry site of *L. monocytogenes* in the human body following ingestion of contaminated food, which is often stored at improper cooling conditions (~10 °C). For the infection of HEPG2 and THP1 cells, bacterial isolates were cultivated for 16 h at 37 °C. OD_{600} was measured and adjusted to OD_{600} 0.1 in 5 ml BHI-Y, and incubated for 2 h at 37 °C. After ingestion and traversing the intestinal epithelium, before hepatocytes and macrophages are infected, *L. monocytogenes* circulates in the human body at 37 °C. The incubation at 10 °C was therefore omitted.

Bacterial cultures were diluted to a multiplicity of infection of 25 and monolayers of cells (~2×10^5 Caco2 cells/well and ~1×10^6 HEPG2/THP1 cells/well) were infected for 1 h at 37 °C.

CFU were determined by plating serial dilutions on TSA. The invasion efficiencies were calculated as CFU recovered after 45 min of incubation in gentamicin-containing medium divided by the mean CFU of the inoculum. The intracellular growth coefficient was determined as follows: IGC = (intracellular $bacteria_{4h}$ − intracellular $bacteria_{45min}$) / intracellular $bacteria_{45min}$. Each experiment was performed in duplicates and repeated at least three times.

2.6. RNA isolation and qRT-PCR

For RNA isolation, single colonies of *L. monocytogenes* were inoculated in 8 ml TSB-Y and either cultivated for 8 h at 37 °C shaking at 150 rpm first and subsequently for 16 h at 10 °C or only cultivated for 16 h at 37 °C shaking at 150 rpm.

Each bacterial culture was adjusted to an OD_{600} 0.1 in 10 ml BHI-Y, incubated for 2 h at 37 °C without shaking and centrifuged at 8000*g* for 5 min at room temperature. The pellets were resuspended in 650 µl warm PM1 solution from the RNeasy PowerMicrobiome Kit (Qiagen) with 25 µl of 2 M DTT (Thermo Scientific). The solution was transferred to PowerBead tubes (Qiagen) and cells were disrupted with a FastPrep-24 5G instrument (MP Biomedicals) using the CoolPrep adapter with the following parameters: six times 45 s at 4.5 m/s Subsequent RNA extraction was carried out using the RNeasy PowerMicrobiome Kit (QIAGEN) according to the manufacturer's instructions but without the on column DNase digestion. RNA was eluted using two times 25 µl RNase-free water. The remaining DNA was digested using the Turbo DNA-free Kit (Life Technologies, Agilent) according to the manufacturer instructions. To confirm the absence of DNA contaminants, 16S rRNA gene PCR was performed using the primers 27F and 1492R (Quijada et al., 2022) (Table S4) and Platinum Taq DNA Polymerase, DNA-free (Thermo Scientific). PCR cycling conditions were as follows: initial denaturation for 2 min at 94 °C; 35 cycles of denaturation for 30 s at 94 °C, annealing for 30 s at 52 °C, elongation for 1 min at 72 °C; final elongation for 2 min at 72 °C; hold at 4 °C. RNA concentrations were measured using the Qubit RNA Broad Range Assay Kit (Thermo Scientific). RNA amounts of 500 ng were used for cDNA synthesis using the RevertAid H Minus First Strand cDNA Synthesis Kit (Thermo Scientific) according to the manufacturer's protocol.

qRT-PCR primers targeting the *L. monocytogenes inlA*, *inlB*, *hly*, *actA*, and *prfA* genes were designed using Primer3 (v.0.4.0). For 16S rRNA qRT-PCR, 341f and 518r primers were used (Muyzer et al., 1993) (Table S4). PCR conditions were applied based on Platinum Taq DNA Polymerase, DNA-free (Thermo Scientific) PCR set-up instructions: 1 × PCR Buffer, 250 nM primer forward and reverse, 1.5 mM $MgCl_2$, 0.2 mM dNTP-Mix, 1.25 U Platinum Taq DNA polymerase and 1 µM EvaGreen (Jena Bioscience) in a final volume of 20 µl. 2 µl of cDNA template were used. Cycling conditions for *inlA*, *inlB*, *hly*, *actA*, *prfA* and 16S rRNA were as follows: initial denaturation for 2 min at 94 °C, 45 cycles of denaturation for 30 s at 94 °C and annealing and extension for 1 min at 60 °C. One cycle was carried out for melting curve analysis (60–95 °C, 0.1 °C/s) for 1 min at 95 °C, 30 s at 60 °C and 30 s at 95 °C. All qRT-PCR reactions were performed using an Mx3000P cycler (Stratagene). A dilution series of genomic *L. monocytogenes* MF3999 DNA (1–10^{-6} ng/µl) was used to determine the primer efficiencies (1.91–1.97 for 16S rRNA, 1.90–1.91 for *inlA*, 1.90–1.95 for *inlB*, 1.90 for *actA*, 1.91–1.92 for *hly*, 1.87–1.90 for *prfA* and 1.91 for *srtA*). Data were analyzed using Mx3000P MxPro software (Stratagene). Each sample was measured in duplicate, and relative quantification was performed using the comparative Ct method. Values, given as x-fold of EGDe, were normalized to 16S rRNA. Mean values ± standard deviation (SD) of three biological replicates measured in duplicates were calculated.

2.7. Cell wall protein isolation and Western Blot

The subcellular fractionation of *L. monocytogenes* was performed according to Monk et al. with slight modifications (Monk et al., 2004). Single colonies of *L. monocytogenes* were inoculated in 20 ml BHI at 37 °C for 16 h shaking at 150 rpm. The cultures were harvested by centrifugation at 5000*g* for 10 min at room temperature. The pellets were resuspended in 1 ml wash buffer (10 mM Tris-HCl, 10 mM $MgCl_2$, pH 6.9) and centrifuged at 12,000*g* for 10 min at room temperature. The pellets were washed with 1 ml wash buffer supplemented with 0.5 M sucrose and centrifuged at 12,000*g* for 10 min at room temperature. The supernatants were discarded and an additional centrifugation step was performed to remove all supernatant. The pellets were resuspended in 500 µl wash buffer supplemented with 0.5 M sucrose, 10 mg/ml lysozyme, 250 U/ml mutanolysin and 10 mM phenylmethanesulfonyl fluoride and incubated for 1.5 h at 37 °C shaking at 400 rpm. The lysates were centrifuged at 12,000*g* for 10 min at room temperature and the supernatants containing the cell wall protein fraction were retained. Protein concentrations were determined using the Pierce BCA Protein Assay Kit (Thermo Scientific). The samples were diluted to a final concentration of 1 mg/ml in NuPAGE LDS Sample Buffer (Invitrogen) and boiled for 5 min at 95 °C shaking at 400 rpm. Equal volumes of cell wall protein fraction samples (10 µg) were loaded onto a NuPAGE 10 % Bis-Tris Mini Protein Gel (Invitrogen). Following electrophoresis (1 h at 200 V), the proteins were blotted onto a nitrocellulose membrane using the iBlot dry blotting system (Invitrogen). The membrane was blocked in Tris-buffered saline with Tween (TBS-T) with 2 % Amersham ECL blocking agent (Cytiva) for 1 h at room temperature and incubated with primary mAb2B3 mouse-anti-InlA antibody (kind gift from Hui Ma, Dublin City University, Ireland) diluted 1:1000 in TBS-T over night at 4 °C. The membrane was washed 2 × 5 min with TBS-T and incubated with secondary ECLPlex goat-anti-mouse IgG-Cy3 antibody (GE Healthcare) diluted 1:2500 in TBS-T for 1 h at room temperature and then washed 4 × 5 min with TBS-T. The protein bands were visualized using the G:BOX gel documentation system (Syngene).

2.8. Statistical analysis

Statistical analysis was performed using IBM SPSS.27. The normality of data sets was checked with histograms and the Shapiro-Wilk-test. If possible, data were normalized with log transformation. The homoscedasticity of data was checked with the Levene and Welch test. Normally distributed data were investigated with one-way ANOVA followed by a Tukey Honest Significant Differences test for homogeneous variances and the Games-Howell test for inhomogeneous variances as post-hoc test. Non-normally distributed data were analyzed with the Kruskal-Wallis rank sum test. $p < 0.05$ was considered as statistically significantly different.

3. Results

3.1. The virulence gene diversity is heterogeneous among lineage I and lineage II isolates

We analyzed the diversity of 99 virulence genes of 767 *L. monocytogenes* isolates from the Norwegian meat and salmon processing industry (Figs. 1, S3, Tables S1–3). The isolates were assigned to 28 CCs, among which 12.5 % belonged to lineage I ($n = 96$) and 87.5 % belonged to lineage II ($n = 671$, Tables 1, S1). Of all lineage I isolates, 24 % ($n = 23$) were collected from meat processing factories, and 76 % ($n = 73$) from salmon processing factories. In contrast, of all lineage II isolates, 65 % ($n = 437$) were isolated from meat processing factories, and 35 % ($n = 234$) from salmon processing factories. The five most commonly isolated CCs from meat and salmon processing factories were CC9, CC7, CC19, CC121 and CC415 (all lineage II), and CC121, CC1, CC7, CC403 and CC19 (all lineage II but CC1), respectively.

The BLAST search revealed that 71 of the virulence genes were present in all isolates (core virulence genes) and 28 of the virulence genes were only harbored by a subset of isolates (accessory virulence genes, Table S2). Length differences of the nucleotide and protein sequences relative to the query (referred to length polymorphisms) were analyzed but not the nucleotide or amino acid composition. Different length polymorphisms were observed for seven core virulence genes (*actA*, *clpE*, *iap*, *inlA*, *inlB*, *inlK*, *lntA* and *oatA*), and five accessory virulence genes (*ami*, *inlJ*, *inlL* and *vip*). Phylogenetically closely related CCs showed similar virulence gene profiles. Overall, CCs of lineage II harbored more accessory virulence genes than CCs of lineage I.

Analysis of a data set containing 111 publicly available Norwegian

human clinical *L. monocytogenes* isolates collected between 2010 and 2015 (Fagerlund et al., 2022a; Walle et al., 2018) revealed that 21.6 % of isolates belonged to lineage I and 78.4 % to lineage II. CC7 was the most prevalent CC, accounting for 23 % ($n = 30$) of the reported listeriosis cases, followed by CC121 (13 %), CC8 (8 %), and CC1 (6 %). CC59, CC87 (both lineage I), CC89 and CC226 (both lineage II) were exclusively isolated from human clinical listeriosis cases and not found among the isolates from the processing environments, whereas CC2, CC315 (both lineage I), CC21 and CC200 (both lineage II) were not found among clinical isolates. The remaining 24 CCs were isolated from both sources. The minimum number of allelic differences obtained by wgMLST analysis between clinical isolates and isolates from the meat and salmon processing industry of the same CC varied from 4 (within the CC19 isolates) to 751 (within the CC31 isolates) (Fig. S4).

The virulence gene profiles of CCs isolated from human clinical listeriosis cases did not differ substantially from isolates collected from food processing environments in this study (Table S5).

3.1.1. *Listeria pathogenicity islands*

The genomic island LIPI-1 was present in all CCs. However, several CCs of both lineage I and II isolated from different meat and salmon processing factories harbored a shorter *actA* (resulting in 604 aa instead of 639 aa) compared to EGDe, due to a 35 aa deletion in the tandem repeat region (aa position 291–325; Figs. 1, S3, S5A, Table S3). LIPI-3 was only present in CCs of lineage I (CC1, CC3, C4 and CC6) isolated from different meat and salmon processing factories. LIPI-4 was predominantly present in lineage I CCs (CC4, CC88, CC220 and CC315) but also in one lineage II CC (CC37). Most of the LIPI-4 positive isolates (24 of 29 isolates) were sampled in the same salmon processing factory (S6). The other five isolates were collected from salmon processing factory S2 and three meat processing factories (M1, M4 and M9, Table S1).

3.1.2. *InlA and inlB*

Six different mutation types were observed in the *inlA* gene leading to PMSCs and hence truncated proteins with different lengths (Table 2, Fig. S5B). *InlA* mutation type 1 (resulting in 605 aa) was present in all CC5 isolates ($n = 13$) collected from the same meat processing factory (M6). Mutation type 4 (8 aa) was present in all CC31 and CC199 isolates (both $n = 3$) collected from three different salmon processing factories (S2, S4 and S6) and one meat processing factory (M8), respectively. Of the 86 CC121 isolates, 80 harbored *inlA* mutation type 6 (491 aa), whereas six isolates (6.98 %) encoded a full-length protein (800 aa). The isolates carrying an *inlA* PMSC mutation were collected from six different meat processing (M1, M3, M4, M6, M7 and M8) and four different salmon processing factories (S2, S4, S5 and S6), while all the isolates carrying the full-length version of the gene were collected from meat processing factory M4. CC121 was the second most common CC with 13.5 % of all analyzed clinical isolates. All isolates also harbored *inlA* mutation type 6.

All 289 CC9 isolates were exclusively collected from meat processing factories and carried a PMSC *inlA* mutation in four variations: two isolates, both collected from M7, harbored mutation type 4 (0.7 %), 152 isolates, collected from M4 (54.6 %), M1 (41.4 %), M3 and M9 (both 2 %), harbored mutation type 11 (684 aa, 52.4 %), 134 isolates, collected from M4 (42.5 %), M1 (38.8 %), M8 (10.5 %), M3 (3.7 %), M5 (3%), M7 and M9 (both 0.75 %), harbored mutation type 12 (576 aa, 46.4 %) and one isolate harbored mutation type 13 (526 aa, 0.3 %). Of the two clinical CC9 isolates (1.8 % of all clinical isolates), one harbored a full-length *inlA* and the other one harbored *inlA* mutation type 12.

In addition, a previously described 797 aa long InlA with an internal deletion of three amino acids at position 738–740 was observed in all CC315 ($n = 10$) collected from salmon processing factory S6 and all three CC6 isolates collected from two different meat processing factories (M4 and M9). This aa deletion between the *Listeria*-Bacteroides repeat domains and the C-terminal LPXTG cell wall anchor did not affect any assigned protein domains (Kovacevic et al., 2013). In contrast to the PMSC mutations, isolates harboring this 3-codon deletion (3CD) mutation are more prevalent among clinical isolates than food isolates and appear to show increased *in vitro* virulence relative to isolates harboring the wildtype allele (Kovacevic et al., 2013; Upham et al., 2019).

All CC5 isolates were collected from the same meat processing factory (M6) and harbored a shorter *inlB* encoding a protein with an internal deletion of amino acids 355–401, resulting in a total length of 583 instead of 630 aa (Table 2, Fig. S5C). This deletion resulted in a shorter *Listeria*-Bacteroides repeat domain (34 instead of 65 aa) and one shorter GW-repeat domain (65 aa instead of 69 aa), while the other two GW-repeat domains were not affected. In contrast, the two clinical CC5 isolates harbored an intact *inlAB* locus.

3.1.3. *Accessory internalin genes*

We observed variations in the occurrence of *inlC2DE*, *inlGC2DE* and *inlGHE*. All isolates harbored one of these three loci. *InlC2DE* was predominantly found in CCs belonging to lineage I but also in some lineage II CCs, whereas *inlGC2DE* was almost exclusively found in lineage II CCs and only in one lineage I CC. *InlGHE* was only present in CC9 isolates (all collected from meat processing factories; Figs. 1, S3, Table S3). The effect of these variations on virulence is unknown. Only the role of the soluble InlC, which mediates intercellular spread and modulates the host innate immune system, has so far been described (Gouin et al., 2010; Ireton et al., 2021).

InlF, which contributes to the crossing of the blood-brain barrier, and *inlJ*, enhancing adhesion (Sabet et al., 2008), were only present in CCs of lineage II. A shorter *inlJ* was present in CC4 (isolated from M4) and CC88 (isolated from S2 and S6, encoding 846 aa instead of 851 aa) due to a five aa deletion at position 798–802 in the unassigned region between the last of four MucBP domains and the C-terminal LPXTG cell wall anchor motif (Fig. S5D).

InlK, which is involved in autophagy escape of *L. monocytogenes* (Dortet et al., 2012), was detected in different length polymorphisms: the full-length protein (598 aa), five longer proteins (600, 602, 604, 606 and 608 aa) and one shorter protein (592 aa; Table S3, Fig. S4E). The length polymorphisms were observed in a stretch of PT/PD repeats starting at position 515 in the C-terminus.

InlL, which is involved in adhesion to mucin (Popowska et al., 2017), was only present in lineage II CCs in two length polymorphisms (Table S3). CC19 and CC403 harbored a protein encoding 621 aa. All CC403 isolates and almost half of the CC19 isolates were collected from salmon processing factory S6, whereas the other CC19 isolates were collected from different meat processing factories (M1, M4 and M6). This length polymorphism was characterized by deletions in the C-terminus: a 1 aa deletion at position 542, a 5 aa deletion at position 549–553 and a 1 aa insertion at position 570 (Fig. S5F).

Table 2
Overview of *inlA* and *inlB* mutation types.

Gene	Mutation type	CC	Distribution among the clonal complex in this study
inlA	PMSC mutation type 1 (605 aa)	CC5	All isolates (n = 13)
	PMSC mutation type 4 (8 aa)	CC31	All isolates (n = 3)
		CC199	All isolates (n = 3)
		CC9	0.7 % of the isolates (n = 2 of 289)
	PMSC mutation type 6 (491 aa)	CC121	93.02 % of the isolates ($n = 80$ of 86)
	PMSC mutation type 11 (684 aa)	CC9	52.4 % of the isolates ($n = 152$ of 289)
	PMSC mutation type 12 (576 aa)	CC9	46.4 % of the isolates ($n = 134$ of 289)
	PMSC mutation type 13 (526 aa)	CC9	0.3 % of the isolates (n = 1 of 289)
	3-Codon deletion (797 aa)	CC315	All isolates (n = 10)
		CC6	All isolates (n = 3)
inlB	Internal deletion of 47 codons (583 aa)	CC5	All isolates (n = 13)

The internalin genes *inlP1* and *inlP3* were detected in all isolates of CC19 and CC403 (both lineage II), present in a previously described hypervariable genetic hotspot of *L. monocytogenes* between the homologs of the mutually conserved core genes *lmo2025* and *lmo2026* (encoding InlL). Both genes were described to contribute to the invasion of intestinal epithelial Caco2 cells *in vitro* (Harter et al., 2019).

3.1.4. Length polymorphisms of other virulence genes

The autolysin-encoding gene *ami*, which contributes to adhesion (Milohanic et al., 2001), was present in all lineage II CCs, but absent in all lineage I CCs except CC3 and CC5. An *ami* gene encoding 588 instead of 917 aa was detected in both CC88 isolates (lineage I, collected from S2 and S6) and one isolate of CC7 (lineage II, collected from S1, Fig. S5G). This length polymorphism was also present in both clinical CC88 isolates and one CC7 isolate and lacked the last 329 aa of the C-terminus, harboring only four GW-repeat domains instead of eight. Another autolysin-encoding gene *aut*, required for entry into host cells (Cabanes et al., 2004), was present in all CCs assigned to lineage II and CC3, CC5, CC11, CC88 and CC101 assigned to lineage I. The isolates belonging to the other CCs of lineage I (CC1, CC2, CC220, CC315, CC4 and CC6) harbored the autolysin-encoding gene *ispC*, also involved in bacterial adhesion (Wang and Lin, 2008), instead of *aut*.

The ATPase-gene *clpE* was present in two different length polymorphisms. One encoded 724 aa like EGDe and was harbored by all isolates of all CCs of lineage II. The other one, which encoded 722 aa due to a 2 aa deletion at position 77–78, was harbored by all lineage I CCs (Fig. S5H). The deletion occurred in an unassigned region of the N-terminus and did not affect the conserved protein domain of the ATP-dependent protease, which is involved in cell division and virulence (Nair et al., 1999).

The *gtcA* gene, which encodes a cell wall teichoic acid glycosylation protein (Promadej et al., 1999), was present in all lineage II CCs but only in some lineage I CCs without an evident correlation with the source of isolation.

Different length polymorphisms were furthermore detected for the invasion-associated secreted endopeptidase gene *iap*, which encodes a characteristic, highly variable central domain containing a stretch of TN repeats (Fig. S5I, Table S3) (Wuenscher et al., 1993). The *lapB* gene, encoding a LPXTG surface adhesion (Reis et al., 2010), was present in all CCs of both lineages except for CC31 (lineage II).

The *lntA* gene, encoding the *Listeria* nuclear targeted protein A, which modulates immune responses *via* heterochromatin formation (Lebreton et al., 2011), was present in two length polymorphisms. While CC5 and CC88 (both lineage I) isolated from one meat and two salmon processing factories, respectively, harbored a *lntA* gene encoding 207 aa, all other CCs harbored one encoding 205 aa like the query sequence of EGDe (Fig. S5J). This N-terminal variation in form of a 2 aa insertion at position 56–57 has previously been described (Lebreton et al., 2014).

The peptidoglycan *O*-acetyltransferase gene *oatA*, involved in immune escape (Aubry et al., 2011), was present in two different length polymorphisms, one of which encoded 622 aa like the query sequence of EGDe and a longer one which encoded 628 aa. Accordingly, the 622 aa protein was present in all CCs belonging to lineage II. The longer OatA was present in all CCs belonging to lineage I and showed a 2 aa insertion at position 433 and a 4 aa insertion at position 443 (Fig. S5K). Neither the acetyltransferase domain nor the YrhL-like hydrolase domain was affected by the insertions (Aubry et al., 2011).

The virulence protein gene *vip*, required for the entry in several mammalian cells (Cabanes et al., 2005), was either present in full-length encoding 399 aa like the query sequence of EGDe or absent in CCs of lineage II. All lineage I CCs harbored a longer *vip* gene encoding 418 aa except CC4, which harbored a *vip* gene encoding 414 aa (Fig. S5L). The longer proteins were characterized by a 14 aa insertion at position 289 (proline rich region) as well as a duplication of 4 aa at position 369 between the proline rich region and the C-terminal LPXTG cell wall anchor (not CC4) and a 1 aa insertion at position 384 (Cabanes et al., 2005).

3.2. The in vitro virulence potential of 13 CCs isolated from the Norwegian meat and salmon processing industry is diverse

We characterized the invasion efficiency of 13 CCs, each represented by three to six isolates ($n = 49$ in total, Table 1, Fig. S2), in human intestinal epithelial Caco2 cells. *L. monocytogenes* EGDe was included as a reference. The invasion efficiency of the 13 CCs ranged from 0 % (under detection limit) for CC5 to 1.43 % for CC403 (Fig. 2A). Significant differences between the invasion efficiencies of the CCs are presented in Table S6. Three CCs were unable to invade Caco2 cells: CC5, CC9 and CC14. The CC5 isolates carried the *inlA* PMSC mutation type 1 (Fig. 2B). All four CC9 isolates encoded truncated variants of InlA (PMSC mutation types 11, 12 and 13). In contrast, the CC14 isolates harbored a full-length *inlA* gene (Fig. 2B). CC3, CC8 and CC121 showed a significantly lower invasion efficiency compared to CC403 and CC415, which showed the highest invasion efficiency (Table S6). Isolates of CC3 and CC8 encoded a full-length *inlA* gene, whereas CC121 was represented by four isolates harboring *inlA* PMSC mutation type 6 and one isolate with a full-length *inlA* gene. CC403 harbored a genetic islet between the homologs of the mutually conserved core genes *lmo2025* and *lmo2026* encoding among other genes *inlP1* and *inlP3*. The increased invasion of CC415 might be due to the presence of the accessory virulence genes *inlF*, *inlJ*, *inlK*, *inlL* and *vip*.

3.3. In-depth characterization of the in vitro virulence of CC14 isolates reveals discrepancy between genotype and phenotype

As the CC14 isolates were unable to invade human intestinal epithelial Caco2 cells, but harbored all essential virulence factors, we determined the invasion efficiency and intracellular proliferation in human intestinal epithelial Caco2 cells, HEPG2 hepatocytes and macrophage-like THP1 cells using two CC14 isolates (MF7668 and MF3999, differentiated by 72 wgMLST allelic differences) and EGDe as a reference. While there was no significant difference between the CC14 isolates and EGDe regarding the internalization into THP1 cells, the invasion efficiency of both CC14 isolates was lower in Caco2 and HEPG2 cells compared to EGDe (Fig. 3A). The invasion efficiency was significantly different for both CC14 isolates in Caco2 cells compared to EGDe, whereas in HEPG2 cells, a significant effect was only observed for isolate MF3999. In contrast, both CC14 isolates displayed a significantly higher intracellular proliferation than EGDe in Caco2 and THP1 cells, whereas only MF3999 showed a significantly higher intracellular proliferation in HEPG2 cells compared to EGDe (Fig. 3B).

Gene expression analysis under conditions used for the infection of Caco2 cells revealed a significantly lower *inlA* and *inlB* gene expression in the two CC14 isolates compared to EGDe, whereas *prfA*, *actA* and *hly* gene expression was not altered (Fig. 3C, Table S7). Analysis under conditions used for the infection of HEPG2 and THP1 cells resulted in a similar gene expression profile (Fig. S6). We also compared the intergenic region between the upstream gene *lmo0433* and the *inlAB* locus (680 bp) of the CC14 isolates and EGDe for differences in PrfA- and SigB-dependent promoter sequences according to Lingnau et al. (1995). A single nucleotide deletion downstream of the SigB-dependent P4 promoter was present in all CC14 isolates (Fig. S7).

3.4. The reconstruction of the inlA gene only affects the in vitro virulence of CC121, but not of CC9 isolates

To study the effect of the *inlA* PMSCs on the invasion efficiency of *L. monocytogenes*, we generated mutants harboring a full-length *inlA* gene by reversing the PMSC mutations for CC9 and CC121 isolates. We included two CC9 isolates with the most prevalent PMSC mutation types: MF4997 harboring *inlA* mutation type 11 (PMSC after 684 aa) and MF6316 harboring *inlA* mutation type 12 (PMSC after 576 aa), and one

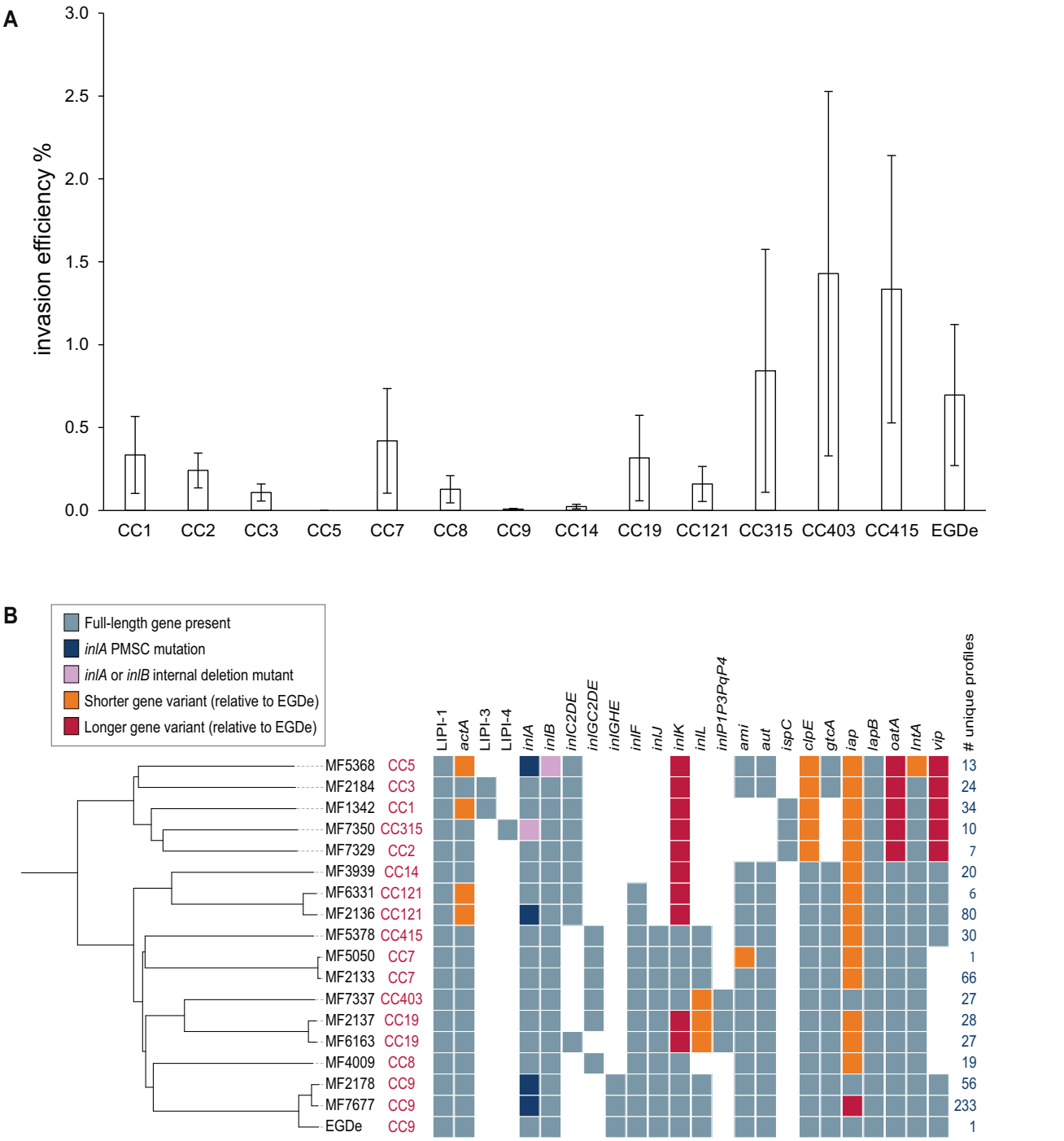

Fig. 2. *In vitro* virulence of 13 CCs isolated from Norwegian food chains. (A) Invasion efficiency (%) into human intestinal epithelial Caco2 cells determined by cocktails of representative isolates (n = 3–6 for each CC). Data are shown as mean value ± SD of four biological replicates determined in duplicate. Statistically significant differences are presented in Table S6. (B) Virulence genes profile of isolates included in the virulence assay. The profile of one representative isolate is shown if isolates of the same CC harbor identical variants. The number of isolates represented by each profile is listed in the last column.

CC121 isolate: MF7707 harboring *inlA* mutation type 6 (PMSC after 491 aa). WGS of the reconstructed *inlA* mutants excluded any additional mutations except the desired gene replacement.

We determined the invasion efficiency for wildtypes and reconstructed *inlA* mutants in human intestinal epithelial Caco2 cells and HEPG2 hepatocytes and included EGDe as a reference (Fig. 4A, B, Table S8). All three wildtype isolates harboring a truncated *inlA* gene were unable to invade Caco2 cells. Reconstruction of *inlA*, resulting in full-length InlA, only enabled the CC121 isolate to invade Caco2 cells, whereas the CC9 isolates remained non-virulent. As expected, reconstruction of *inlA* did not significantly affect the invasion into HEPG2 cells, as it is predominantly dependent on the interaction between InlB and c-Met.

Virulence gene expression analysis revealed no significant difference in *inlA*, *inlB* and *prfA* gene expression between the wildtypes and the corresponding reconstructed *inlA* mutants under growth conditions used for the infection of Caco2 cells (Fig. 4C–E, Table S8). However, *inlA* gene expression was significantly lower in both CC9 wildtypes and one reconstructed *inlA* CC9 mutant compared to EGDe, whereas *inlB* expression was only significantly lower in the CC9 MF6316 wildtype and

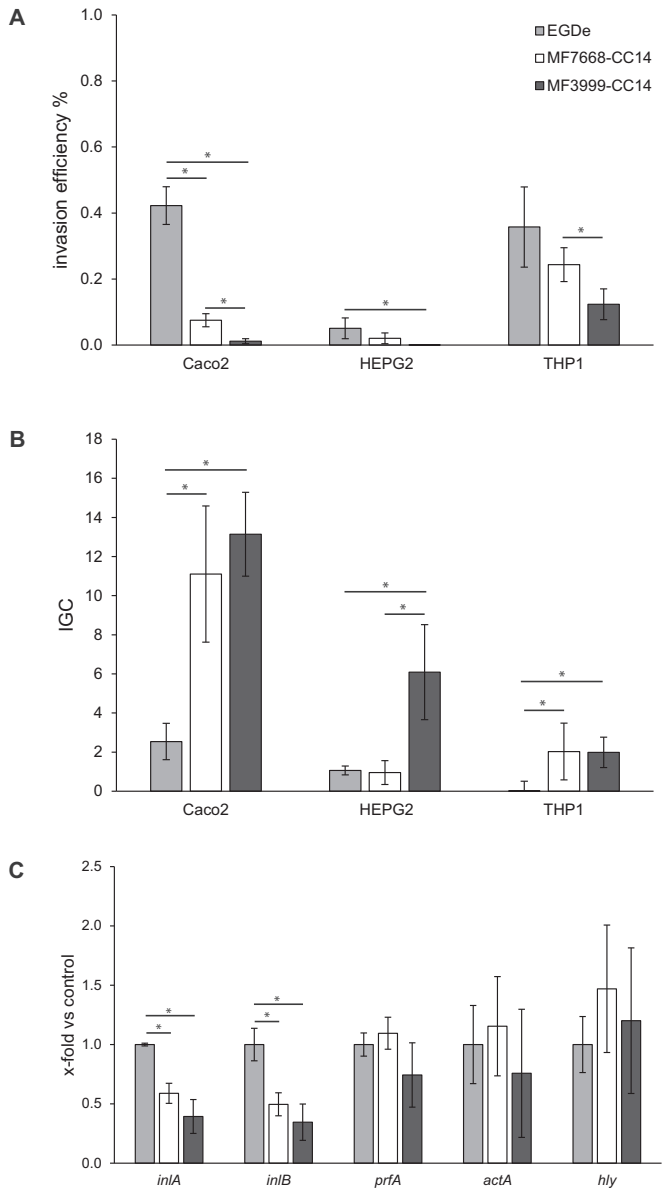

Fig. 3. *In vitro* virulence of CC14 isolates. (A) Invasion efficiency (%) of EGDe (light grey), MF7668-CC14 (white) and MF3999-CC14 (dark grey) into human intestinal epithelial Caco2 cells, HEPG2 hepatocytes and macrophage-like THP1 cells. (B) Intracellular proliferation, represented as intracellular growth coefficient (IGC), in Caco2, HEPG2 and THP1 cells. (C) *InlA*, *inlB*, *prfA*, *actA* and *hly* gene expression of EGDe (control, light grey), MF7668 (white) and MF3999 (dark grey). Data are shown as mean value ± SD of three biological replicates determined in duplicate. *Statistically significant difference between the isolates ($p < 0.05$).

reconstructed *inlA* mutant compared to EGDe (Table S8). Under growth conditions used for the infection of HEPG2 and THP1 cells, we observed a significantly lower *prfA* expression in the CC9 MF4997 reconstructed *inlA* mutant compared to the wildtype (Fig. S8, Table S8). Comparison of the intergenic region between the upstream gene *lmo0433* and the *inlAB* locus revealed no differences in the PrfA- and SigB-dependent promoter regions (Fig. S7).

In contrast, Western Blot analysis showed that InlA was only present in the cell wall of EGDe and the CC121 reconstructed *inlA* mutant, whereas it not detectable in the two CC9 reconstructed *inlA* mutants (Figs. 4F, S8D). This shows that reconstruction of the truncated *inlA* with the sequence encoding full-length InlA did not result in InlA protein exposure on the cell surface in the two CC9 isolates, thereby potentially explaining why the CC9 reconstructed *inlA* mutants failed to invade Caco2 cells. Gene expression analysis of *srtA*, which is identical in all isolates, revealed no significant differences between EGDe, the wildtypes and the corresponding reconstructed *inlA* mutants under growth conditions used for the infection of Caco2 cells (Fig. 4G). *srtA* encodes the enzyme Sortase A that anchors InlA to the cell wall by processing and covalent linkage to the peptidoglycan. In addition, a comparison of the N-terminal signal peptide sequence revealed no differences between the wildtypes, the reconstructed *inlA* mutants and EGDe.

4. Discussion

In this study, whole genome sequences of 767 *L. monocytogenes* isolates collected over three decades from 15 Norwegian meat and salmon processing factories were characterized using comparative genomic analyses. For 13 major CCs, the virulence gene profile was compared with *in vitro* virulence data to broaden the understanding of *L. monocytogenes* pathogenicity and to evaluate the application potential of WGS in risk assessment in the food industry.

The prevalence of the 28 detected CCs in the two Norwegian food sectors was similar to the global distribution of *L. monocytogenes* in food chains. The vast majority comprised lineage II isolates belonging to CC9, CC121 and CC7, which have previously been described to be persistent, pervasive and hypovirulent. Isolates of lineage I belonging to CC1, CC6, CC2 and CC4 were also detected, although to a lesser extent, and have previously been classified as hypervirulent (Maury et al., 2016; Painset et al., 2019). We observed a highly conserved pattern for the virulence genes within each CC. Differences in the virulence gene profiles were limited to length polymorphisms and not extended to differences in nucleotide and amino acid composition. The observed length polymorphisms are most likely due to phylogenetic relationships. However, the effect of length polymorphism except truncations on the functionality of virulence factors is largely unknown.

Accessory sets of genes that have been reported to contribute to hypervirulence, like LIPI-3 or LIPI-4, almost exclusively occurred in CCs of lineage I as previously observed (Cotter et al., 2008; Maury et al., 2019; Quereda et al., 2017). In contrast, isolates of lineage II (CC9, CC121, CC199 and CC31) were found to harbor PMSC mutations in the *inlA* gene that lead to a truncated protein. The resulting hypovirulence derived from this genotype has comprehensively been described in different model systems (Maury et al., 2016; Nightingale et al., 2008; Olier et al., 2003; Rychli et al., 2017; Schiavano et al., 2021). Isolates of one lineage I CC, namely CC5, also encoded a PMSC in the *inlA* gene as well as an internal in-frame deletion in the *inlB* gene. Both the *inlA* PMSC mutation type 1 and the internal in-frame deletion mutation in *inlB* were also detected in eight CC5 isolates from Polish meat processing environments and 11 CC5 isolates from Irish meat processing environments, respectively (Hurley et al., 2019; Kurpas et al., 2020). Of note, the two clinical CC5 isolates harbored an intact *inlAB* locus, suggesting an accumulation of these mutations due to clonal spread of CC5 in the same meat processing factory (M6) between 2010 and 2019 rather than a CC-specific characteristic.

One of our aims was to test whether it is possible to predict the virulence potential solely based on MLST/CC classification with the underlying knowledge on the determined genetic virulence profiles. Therefore, we determined the *in vitro* invasion efficiency of 13 CCs in human intestinal epithelial cells, as this route of entry is a prerequisite for *L. monocytogenes* to cause systemic disease in humans. Our results confirmed an expected low invasion efficiency of CC5 and CC9 as the truncated InlA is not exposed on the cell surface and can therefore not interact with E-cadherin on the surface of the human intestinal epithelial cells (Bonazzi et al., 2009). Unexpectedly, CC121 showed a moderate virulence potential comparable to CC8 and CC3, although only one of the five isolates harbored a full-length *inlA* gene.

The presence of LIPI-4 and the 3CD *inlA* variant, which has been

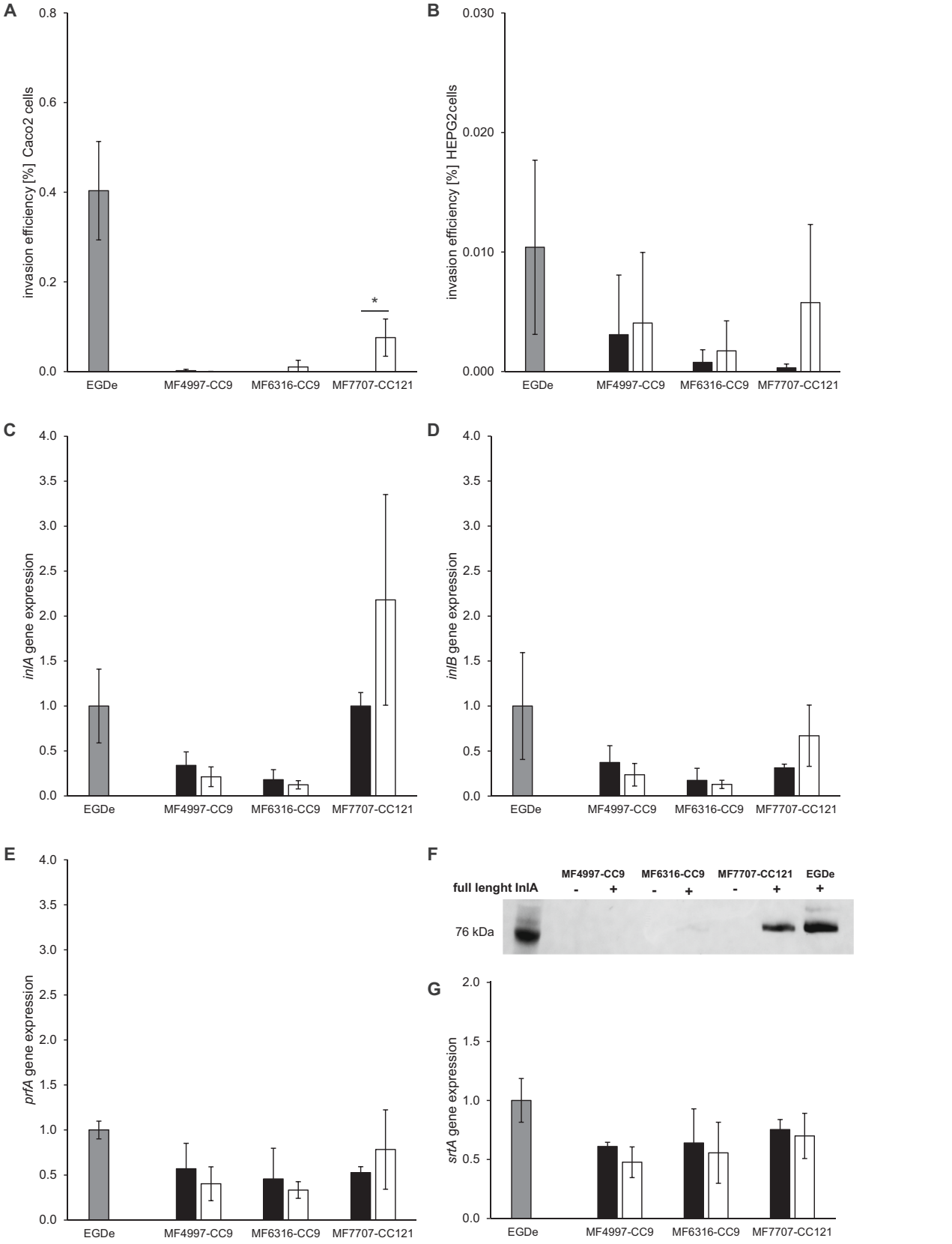

(caption on next page)

Fig. 4. Effect of reconstructed *inlA* in CC9 and CC121 isolates. Invasion efficiency (%) of EGDe (grey), the wildtype isolates (black, harboring a truncated *inlA*) and the reconstructed *inlA* mutants (white) of the two CC9 isolates MF4997 and MF6316, and the CC121 isolate M7707 into (A) human intestinal epithelial Caco2 cells and (B) HEPG2 hepatocytes.
(C) *InlA*, (D) *inlB* and (E) *prfA* gene expression of EGDe (grey), the wildtype isolates (black, harboring a truncated *inlA*) and the reconstructed *inlA* mutants (white) of the two CC9 isolates MF4997 and MF6316 and the CC121 isolate M7707. Data are shown as mean value ± SD of three biological replicates determined in duplicate. *Statistically significant difference between the wildtype and the reconstructed mutant ($p < 0.05$; significant differences between other combinations of isolates are presented in Table S8).
(F) InlA protein expression in the cell wall of EGDe, the wildtype isolates and the reconstructed *inlA* mutants.
(G) *SrtA* gene expression of EGDe (grey), the wildtype isolates (black, harboring a truncated *inlA*) and the reconstructed *inlA* mutants (white) of the two CC9 isolates MF4997 and MF6316 and the CC121 isolate M7707.

associated with increased invasion in CC315 (Kovacevic et al., 2013; Maury et al., 2019; Upham et al., 2019) and the accessory internalin genes *inlP1P3PqP4* in CC403 isolates could likely be responsible for the higher invasion efficiency relative to the reference EGDe. In our study, the presence of LIPI-3 in CC3 did not result in an increased *in vitro* virulence potential in human intestinal epithelial cells compared to EGDe. This was not surprising since the encoded Listeriolysin S is only highly expressed *in vivo* in murine models and alters the host intestinal microbiota, thereby facilitating the colonization of the intestine (Cotter et al., 2008). CC9, CC121 and CC415 were the only CCs harboring a combination of the accessory virulence genes *inlF*, *inlJ*, *inlK*, *inlL* and *vip*. In contrast to CC9 and CC121, CC415 encoded a full-length InlA. The combination of all of these accessory virulence genes in CC415 was suggested to be an indication of a highly virulent phenotype and this was in accordance with our obtained results. We expected intermediate virulence phenotypes for CC1, CC2, CC7, CC8, CC14 and CC19 due to CC-specific combinations of virulence genes. This was confirmed by our *in vitro* experiments for all afore-mentioned CCs except for CC14, which surprisingly showed a non-virulent phenotype. This is in contrast to a previous study, reporting hypervirulence for this CC (Cardenas-Alvarez et al., 2019). As the phenotype we observed could not be explained by the virulence gene profile, we performed virulence gene expression analysis and detected a significantly lower *inlA* and *inlB* gene expression compared to EGDe as a reference, possibly due to a point mutation in the promoter region.

Our attempt to reconstruct the full-length *inlA* gene in isolates of CC9 and CC121, that harbored different PMSC mutations, only resulted in InlA functionality in the CC121 isolate but not in CC9 isolates. Also Olier et al. reported a necessary but not sufficient role of restored InlA in *in vivo* infection of *L. monocytogenes* in chick embryos (Olier et al., 2005). We conclusively showed that the observed phenotype in CC9 isolates was due to the lack of InlA exposure in the cell wall, which is a prerequisite for the interaction with E-cadherin on the surface of epithelial cells. As the expression of the *srtA* gene, encoding Sortase A, which covalently links InlA to the peptidoglycan after processing, as well as the N-terminal signal peptide sequence were identical in the CC9 and CC121 wildtypes and reconstructed *inlA* mutants, possible explanations could be translational regulation, intracellular degradation or a secretion pathway defect. Our study clearly demonstrates that the mere presence of a functional *inlA* gene is not sufficient for virulence, but gene and protein expression and the presentation of InlA on the cell wall are required.

Although the virulence gene profiles were highly conserved within the individual CCs, a prediction of virulence potential based on MLST/CC classification is rather challenging and only possible if genotypic and phenotypic data are linked. In the case of a CC like CC121, that is generally associated with *inlA* truncation mutations and hypovirulence, a MLST/CC-based prediction would have been misleading without further genotypic and phenotypic investigations revealing that approximately 7 % of the CC121 isolates in this study harbored an intact *inlA* gene. CC121 has in fact been the second most commonly isolated CC from human listeriosis cases in Norway between 2010 and 2015, despite all isolates harboring a truncated *inlA* gene (Fagerlund et al., 2022a). This shows that zero infection risk does not exist for *L. monocytogenes* even though epidemiological and patient data are lacking for these cases. In the case of a CC like CC14, neither a prediction based on MLST/CC classification nor on genotypic results would have been accurate, as the CC did not show *in vitro* virulence. Also CC14 isolates have been isolated from human listeriosis cases in Norway between 2010 and 2015 (Fagerlund et al., 2022a). Of note, *in vitro* virulence assays also have limitations. By this approach, the ability of an isolate to invade cells and hence initiate infection can be estimated and the virulence potential relative to a reference can be evaluated. But we also have to consider other variables that cannot be reproduced by using simplistic *in vitro* models, like host factors, infectious doses, infection pathways that are not yet known and the presence of innate microbiota among many others.

With the advent of WGS, the possibility to perform risk assessment in a targeted direction on subpopulations of pathogenic foodborne bacteria like *L. monocytogenes* to support decision making in the food industry is under discussion (Buchanan et al., 2017; Franz et al., 2016; UCD Centre for Food Safety Ireland et al., 2018). However, the implementation of this approach is challenging. It will be demanding to assess and classify the risk regarding the likelihood of illness based on WGS data and resulting gene profiles for *L. monocytogenes* that can easily transition from a saprophytic to a pathogenic lifestyle. Ideally, obtaining profiles of particular marker genes that have unambiguously been associated with a higher or lower risk to cause listeriosis from WGS data would allow the industry to prioritize the resolution of one contamination scenario in the case of multiple contamination scenarios in a factory. The establishment of *L. monocytogenes* virulence profiles suitable for risk assessment in the food industry is anything but trivial as it is ultimately a matter of responsibility. As we have shown, even though truncated InlA evidently correlates with persistence and hypovirulence and could be used as a marker for these characteristics, there are still human listeriosis cases caused by hypovirulent CCs like CC9 and CC121. On the contrary, reconstructed InlA did only partially or not at all lead to re-establishment of the *in vitro* invasion potential and as exemplified by CC14, even a set of functional virulence genes does not automatically entail virulence. Thus, data have to be evaluated carefully as both an underestimation of truncated InlA as well as an overestimation of full-length InlA should be avoided. It is of importance to also consider host factors and susceptibility in regards to risk assessment as highlighted by a study conducted by Maury et al. showing that CC9 and CC121 are more often isolated from highly immunocompromised patients in contrast to CC1, CC2, CC4 and CC6 (Maury et al., 2016).

In contrast to genetic stress and persistence determinants, that are predominantly associated with *L. monocytogenes* isolates from food processing environments but do not occur to the same extent in clinical isolates (Fagerlund et al., 2022a), the virulence gene content appears to remain stable among isolates from food processing environments and clinical isolates. It is relevant to mention that in addition to differences in genetic virulence profiles, other factors like the type of spoiled product, exposure, epidemiology and whether or not the causative CC has been isolated and typed correctly also influence the prevalence of CCs among human clinical listeriosis cases (Disson et al., 2021; Guidi et al., 2021; Maury et al., 2016).

In conclusion, the prediction of the virulence potential based on genotypic data obtained from WGS of *L. monocytogenes* has its limitations, but adds valuable information to risk assessment in the food

industry in combination with phenotypic characterization. However, there are many unsolved mysteries regarding the orchestration and regulation of genes and it is of particular relevance not to neglect phenotypic characterization in the face of the data avalanches that come along with next-generation sequencing technologies. Our study has highlighted the importance of collecting phenotypic data and coupling them to genomic analyses in order to establish sound predictions that can be used for risk assessment of *L. monocytogenes* in the food industry in the near future.

Declaration of competing interest

The authors declare that they have no known competing financial interests or personal relationships that could have appeared to influence the work reported in this paper.

Data availability

The raw data and assembled genomes are available at NCBI under BioProject accessions PRJNA293674 (Fagerlund et al., 2016a), PRJNA419519 (Fagerlund et al., 2020), and PRJNA689484 (Fagerlund et al., 2022b). Raw sequencing data for the *inlA* reconstruction mutants were deposited in the Sequence Read Archive under accessions PRJNA839903.

Acknowledgments

We sincerely thank Charlotte Kummen and Vibeke Høst at Nofima and Elisabeth Frohner and Andreas Zaiser at the University of Veterinary Medicine, Vienna, for excellent technical assistance and Dr. Hui Ma (Dublin City University) for the kind gift of the mAb2B3 mouse-anti-InlA antibodies.

Funding

This work was supported by the Research Council of Norway through grant no. 294910.

Appendix A. Supplementary data

Supplementary data to this article can be found online at https://doi.org/10.1016/j.ijfoodmicro.2022.109962.

References

Arnaud, M., Chastanet, A., Débarbouillé, M., 2004. New vector for efficient allelic replacement in naturally nontransformable, low-GC-content, Gram-positive bacteria. Appl. Environ. Microbiol. 70, 6887–6891. https://doi.org/10.1128/AEM.70.11.6887-6891.2004. Check for updates on crossmark.

Aubry, C., Goulard, C., Nahori, M.-A., Cayet, N., Decalf, J., Sachse, M., Boneca, I.G., Cossart, P., Dussurget, O., 2011. OatA, a peptidoglycan O-acetyltransferase involved in Listeria monocytogenes immune escape, is critical for virulence. J. Infect. Dis. 204, 731–740. https://doi.org/10.1093/infdis/jir396.

Bergholz, T.M., Shah, M.K., Burall, L.S., Rakic-Martinez, M., Datta, A.R., 2018. Genomic and phenotypic diversity of Listeria monocytogenes clonal complexes associated with human listeriosis. Appl. Microbiol. Biotechnol. https://doi.org/10.1007/s00253-018-8852-5.

Bonazzi, M., Lecuit, M., Cossart, P., 2009. Listeria monocytogenes internalin and E-cadherin: from bench to bedside. Cold Spring Harb. Perspect. Biol. 1 https://doi.org/10.1101/CSHPERSPECT.A003087.

Buchanan, R.L., Gorris, L.G.M., Hayman, M.M., Jackson, T.C., Whiting, R.C., 2017. A review of Listeria monocytogenes: an update on outbreaks, virulence, dose-response, ecology, and risk assessments. Food Control 75, 1–13. https://doi.org/10.1016/J.FOODCONT.2016.12.016.

Bucur, F.I., Grigore-Gurgu, L., Crauwels, P., Riedel, C.U., Nicolau, A.I., 2018. Resistance of Listeria monocytogenes to stress conditions encountered in food and food processing environments. Front. Microbiol. https://doi.org/10.3389/fmicb.2018.02700.

Cabanes, D., Dussurget, O., Dehoux, P., Cossart, P., 2004. Auto, a surface associated autolysin of Listeria monocytogenes required for entry into eukaryotic cells and virulence. Mol. Microbiol. https://doi.org/10.1111/j.1365-2958.2003.03945.x.

Cabanes, D., Sousa, S., Cebriá, A., Lecuit, M., García-Del Portillo, F., Cossart, P., 2005. Gp96 is a receptor for a novel Listeria monocytogenes virulence factor, Vip, a surface protein. EMBO J. https://doi.org/10.1038/sj.emboj.7600750.

Cardenas-Alvarez, M.X., Townsend Ramsett, M.K., Malekmohammadi, S., Bergholz, T.M., 2019. Evidence of hypervirulence in Listeria monocytogenes clonal complex 14. J. Med. Microbiol. 68, 1677–1685. https://doi.org/10.1099/JMM.0.001076/CITE/REFWORKS.

Ciolacu, L., Nicolau, A.I.A.I., Wagner, M., Rychli, K., 2014. Listeria monocytogenes isolated from food samples from a Romanian black market show distinct virulence profiles. Int. J. Food Microbiol. 209, 44–51. https://doi.org/10.1016/j.ijfoodmicro.2014.08.035.

<collab>EFSA, E.P.on B.H.</collab>, Koutsoumanis, K., Allende, A., Alvarez-Ordóñez, A., Bolton, D., Bover-Cid, S., Chemaly, M., Davies, R., De Cesare, A., Hilbert, F., Lindqvist, R., Nauta, M., Peixe, L., Ru, G., Simmons, M., Skandamis, P., Suffredini, E., Jenkins, C., Malorny, B., Ribeiro Duarte, A.S., Torpdahl, M., da Silva Felício, M.T., Guerra, B., Rossi, M., Herman, L., 2019. Whole genome sequencing and metagenomics for outbreak investigation, source attribution and risk assessment of food-borne microorganisms. EFSA J. 17, e05898 https://doi.org/10.2903/j.efsa.2019.5898.

<collab>UCD Centre for Food Safety Ireland, D.</collab>, Van Hoorde, K., Butler, F., 2018. Use of next-generation sequencing in microbial risk assessment. EFSA J. 16, e16086 https://doi.org/10.2903/j.efsa.2018.e16086.

Cotter, P.D., Draper, L.A., Lawton, E.M., Daly, K.M., Groeger, D.S., Casey, P.G., Ross, R. P., Hill, C., 2008. Listeriolysin S, a novel peptide haemolysin associated with a subset of lineage I Listeria monocytogenes. PLoS Pathog. 4, e1000144 https://doi.org/10.1371/journal.ppat.1000144.

Davis, S., Pettengill, J.B., Luo, Y., Payne, J., Shpuntoff, A., Rand, H., Strain, E., 2015. CFSAN SNP pipeline: an automated method for constructing SNP matrices fromnext-generation sequence data. PeerJ Comput. Sci. 2015, e20 https://doi.org/10.7717/PEERJ-CS.20/SUPP-1.

Disson, O., Moura, A., Lecuit, M., 2021. Making sense of the biodiversity and virulence of Listeria monocytogenes. Trends Microbiol. 29, 811–822. https://doi.org/10.1016/J.TIM.2021.01.008.

Dortet, L., Mostowy, S., Cossart, P., 2012. Listeria and autophagy escape: involvement of InlK, an internalin-like protein. Autophagy 8, 132–134. https://doi.org/10.4161/AUTO.8.1.18218.

Drolia, R., Tenguria, S., Durkes, A.C., Turner, J.R., Bhunia, A.K., 2018. Listeria adhesion protein induces intestinal epithelial barrier dysfunction for bacterial translocation. Cell Host Microbe 23, 470–484. https://doi.org/10.1016/j.chom.2018.03.004.

EFSA Biohaz, Ricci, A., Allende, A., Bolton, D., Chemaly, M., Davies, R., Fernández Escámez, P.S., Girones, R., Herman, L., Koutsoumanis, K., Nørrung, B., Robertson, L., Ru, G., Sanaa, M., Simmons, M., Skandamis, P., Snary, E., Speybroeck, N., Ter Kuile, B., Threlfall, J., Wahlström, H., Takkinen, J., Wagner, M., Arcella, D., Da Silva Felicio, M.T., Georgiadis, M., Messens, W., Lindqvist, R., 2018. Listeria monocytogenes contamination of ready-to-eat foods and the risk for human health in the EU. EFSA J. 16, e05134 https://doi.org/10.2903/J.EFSA.2018.5134.

Fagerlund, A., Langsrud, S., Schirmer, B.C., Moretro, T., Heir, E., 2016a. Genome analysis of Listeria monocytogenes sequence type 8 strains persisting in salmon and poultry processing environments and comparison with related strains. PLoS One 11, e0151117. https://doi.org/10.1371/journal.pone.0151117.

Fagerlund, A., Smith, V., Røhr, Å.K., Lindbäck, T., Parmer, M.P., Andersson, K.K., Reubsaet, L., Økstad, O.A., 2016b. Cyclic diguanylate regulation of Bacillus cereus group biofilm formation. Mol. Microbiol. 101, 471–494. https://doi.org/10.1111/MMI.13405.

Fagerlund, A., Langsrud, S., Møretrø, T., 2020. In-depth longitudinal study of Listeria monocytogenes ST9 isolates from the meat processing industry: resolving diversity and transmission patterns using whole-genome sequencing. Appl. Environ. Microbiol. 86 https://doi.org/10.1128/AEM.00579-20.

Fagerlund, A., Idland, L., Heir, E., Møretrø, T., Aspholm, M., Lindbäck, T., Langsrud, S., 2022a. WGS analysis of Listeria monocytogenes from rural, urban, and farm environments in Norway: genetic diversity, persistence, and relation to clinical and food isolates. Appl. Environ. Microbiol. https://doi.org/10.1128/AEM.02136-21.

Fagerlund, A., Wagner, E., Mretr, T., Heir, E., Moen, B., Rychli, K., Langsrud, S., 2022b. Pervasive Listeria monocytogenes are common in Norwegian food chains and associated with increased prevalence of stress survival and resistance determinants. Appl. Environ. Microbiol. https://doi.org/10.1128/aem.00861-22.

Félix, B., Sevellec, Y., Palma, F., Douarre, P.E., Felten, A., Radomski, N., Mallet, L., Blanchard, Y., Leroux, A., Soumet, C., Bridier, A., Piveteau, P., Ascensio, E., Hébraud, M., Karpíšková, R., Gelbíčová, T., Torresi, M., Pomilio, F., Cammà, C., Di Pasquale, A., Skjerdal, T., Pietzka, A., Ruppitsch, W., Canelhas, M.R., Papić, B., Hurtado, A., Wullings, B., Bulawova, H., Castro, H., Lindström, M., Korkeala, H., Šteingolde, Ž., Kramarenko, T., Cabanova, L., Szymczak, B., Gareis, M., Oswaldi, V., Marti, E., Seyfarth, A.-M., Leblanc, J.-C., Guillier, L., Roussel, S., 2022. A European-wide dataset to uncover adaptive traits of Listeria monocytogenes to diverse ecological niches. Sci. Data 9, 190. https://doi.org/10.1038/s41597-022-01278-6.

Franz, E., Gras, L.M., Dallman, T., 2016. Significance of whole genome sequencing for surveillance, source attribution and microbial risk assessment of foodborne pathogens. Curr. Opin. Food Sci. 8, 74–79. https://doi.org/10.1016/J.COFS.2016.04.004.

Gaillard, J.L., Berche, P., Frehel, C., Gouln, E., Cossart, P., 1991. Entry of L. monocytogenes into cells is mediated by internalin, a repeat protein reminiscent of surface antigens from Gram-positive cocci. Cell 65, 1127–1141. https://doi.org/10.1016/0092-8674(91)90009-N.

Gascuel, O., 1997. BIONJ: an improved version of the NJ algorithm based on a simple model of sequence data. Mol. Biol. Evol. 14, 685–695. https://doi.org/10.1093/oxfordjournals.molbev.a025808.

Gelbíčová, T., Koláčková, I., Pantůček, R., Karpíšková, R., 2015. A novel mutation leading to a premature stop codon in inlA of Listeria monocytogenes isolated from neonatal listeriosis. New Microbiol. 38, 293–296.

Gouin, E., Adib-Conquy, M., Balestrino, D., Nahori, M.A., Villiers, V., Colland, F., Dramsi, S., Dussurget, O., Cossart, P., 2010. The Listeria monocytogenes InlC protein interferes with innate immune responses by targeting the IkB kinase subunit IKKa. Proc. Natl. Acad. Sci. U. S. A. 107, 17333–17338. https://doi.org/10.1073/PNAS.1007765107.

Guidi, F., Orsini, M., Chiaverini, A., Torresi, M., Centorame, P., Acciari, V.A., Salini, R., Palombo, B., Brandi, G., Amagliani, G., Schiavano, G.F., Massacci, F.R., Fisichella, S., Domenico, M.Di, Ancora, M., Pasquale, A.Di, Duranti, A., Cammà, C., Pomilio, F., Blasi, G., 2021. Hypo- and hyper-virulent Listeria monocytogenes clones persisting in two different food processing plants of central Italy. Microorganisms 9, 376. https://doi.org/10.3390/MICROORGANISMS9020376.

Harter, E., Lassnig, C., Wagner, E.M., Zaiser, A., Wagner, M., Rychli, K., 2019. The novel internalins InlP1 and InlP4 and the internalin-like protein InlP3 enhance the pathogenicity of Listeria monocytogenes. Front. Microbiol. 10, 1644.

Hurley, D., Luque-Sastre, L., Parker, C.T., Huynh, S., Eshwar, A.K., Nguyen, S.V., Andrews, N., Moura, A., Fox, E.M., Jordan, K., Lehner, A., Stephan, R., Fanning, S., 2019. Whole-Genome sequencing-based characterization of 100 Listeria monocytogenes isolates collected from food processing environments over a four-year period. mSphere 4. https://doi.org/10.1128/MSPHERE.00252-19/ASSET/A83A600B-E392-4FB2-A7E8-A4A536A03C85/ASSETS/GRAPHIC/MSPHERE.00252-19-F0005.JPEG.

Ireton, K., Mortuza, R., Gyanwali, G.C., Gianfelice, A., Hussain, M., 2021. Role of internalin proteins in the pathogenesis of Listeria monocytogenes. Mol. Microbiol. 116, 1407–1419. https://doi.org/10.1111/MMI.14836.

Janes, B.K., Stibitz, S., 2006. Routine markerless gene replacement in Bacillus anthracis. Infect. Immun. 74, 1949–1953. https://doi.org/10.1128/IAI.74.3.1949-1953.2006.

Jordan, K., Hunt, K., Lourenco, A., Pennone, V., 2018. Listeria monocytogenes in the food processing environment. Curr. Clin. Microbiol. Rep. 52 (5), 106–119. https://doi.org/10.1007/S40588-018-0090-1.

Kaufman, L., Rousseeuw, P.J., 1990. Finding Groups in Data. An Introduction to Cluster Analysis. In: Wiley Series in Probability And Statistics. https://doi.org/10.1002/9780470316801.

Kovacevic, J., Arguedas-Villa, C., Wozniak, A., Tasara, T., Allen, K.J., 2013. Examination of food chain-derived listeria monocytogenes strains of different serotypes reveals considerable diversity in inlA genotypes, mutability, and adaptation to cold temperatures. Appl. Environ. Microbiol. 79, 1915–1922. https://doi.org/10.1128/AEM.03341-12/SUPPL_FILE/ZAM999104200SO1.PDF.

Kurpas, M., Osek, J., Moura, A., Leclercq, A., Lecuit, M., Wieczorek, K., 2020. Genomic characterization of Listeria monocytogenes isolated from ready-to-eat meat and meat processing environments in Poland. Front. Microbiol. 11, 1412. https://doi.org/10.3389/fmicb.2020.01412.

Lebreton, A., Lakisic, G., Job, V., Fritsch, L., Tham, T.N., Camejo, A., Matteï, P.J., Regnault, B., Nahori, M.A., Cabanes, D., Gautreau, A., Ait-Si-Ali, S., Dessen, A., Cossart, P., Bierne, H., 2011. A bacterial protein targets the BAHD1 chromatin complex to stimulate type III interferon response. Science 331, 1319–1321. https://doi.org/10.1126/SCIENCE.1200120.

Lebreton, A., Job, V., Ragon, M., Le Monnier, A., Dessen, A., Cossart, P., Bierne, H., 2014. Structural basis for the inhibition of the chromatin repressor BAHD1 by the bacterial nucleomodulin LntA. MBio 5. https://doi.org/10.1128/MBIO.00775-13/SUPPL_FILE/MBO001141707S1.DOCX.

Lee, S., Chen, Y., Gorski, L., Ward, T.J., Osborne, J., Kathariou, S., 2018. Listeria monocytogenes source distribution analysis indicates regional heterogeneity and ecological niche preference among serotype 4b clones. MBio 9, e00396-18. https://doi.org/10.1128/mBio.00396-18.

Letunic, I., Bork, P., 2021. Interactive Tree Of Life (iTOL) v5: an online tool for phylogenetic tree display and annotation. Nucleic Acids Res. 49, W293–W296. https://doi.org/10.1093/NAR/GKAB301.

Lingnau, A., Domann, E., Hudel, M., Bock, M., Nichterlein, T., Wehland, J., Chakraborty, T., 1995. Expression of the Listeria monocytogenes EGD inlA and inlB genes, whose products mediate bacterial entry into tissue culture cell lines, by PrfA-dependent and -independent mechanisms. Infect. Immun. 63, 3896–3903.

Maechler, M., Rousseeuw, P., Struyf, A., Hubert, M., Hornik, K., 2021. Cluster: Cluster Analysis Basics And Extensions. R Package Version 2.1.2.

Maury, M.M., Tsai, Y.-H., Charlier, C., Touchon, M., Chenal-Francisque, V., Leclercq, A., Criscuolo, A., Gaultier, C., Roussel, S., Brisabois, A., Disson, O., Rocha, E.P.C., Brisse, S., Lecuit, M., 2016. Uncovering Listeria monocytogenes hypervirulence by harnessing its biodiversity. Nat. Genet. 48, 308–313. https://doi.org/10.1038/ng.3501.

Maury, M.M., Bracq-Dieye, H., Huang, L., Vales, G., Lavina, M., Thouvenot, P., Disson, O., Leclercq, A., Brisse, S., Lecuit, M., 2019. Hypervirulent Listeria monocytogenes clones' adaption to mammalian gut accounts for their association with dairy products. Nat. Commun. https://doi.org/10.1038/s41467-019-10380-0.

Meza-Torres, J., Lelek, M., Quereda, J.J., Sachse, M., Manina, G., Ershov, D., Tinevez, J. Y., Radoshevich, L., Maudet, C., Chaze, T., Gianetto, Q.G., Matondo, M., Lecuit, M., Martin-Verstraete, I., Zimmer, C., Bierne, H., Dussurget, O., Cossart, P., Pizarro-Cerdá, J., 2021. Listeriolysin S: a bacteriocin from Listeria monocytogenes that induces membrane permeabilization in a contact-dependent manner. Proc. Natl. Acad. Sci. U. S. A. 118 https://doi.org/10.1073/PNAS.2108155118.

Milohanic, E., Jonquières, R., Cossart, P., Berche, P., Gaillard, J.L., 2001. The autolysin Ami contributes to the adhesion of Listeria monocytogenes to eukaryotic cells via its cell wall anchor. Mol. Microbiol. https://doi.org/10.1046/j.1365-2958.2001.02208.x.

Monk, I.R., Cook, G.M., Monk, B.C., Bremer, P.J., 2004. Morphotypic conversion in Listeria monocytogenes biofilm formation: biological significance of rough colony isolates. Appl. Environ. Microbiol. 70, 6686. https://doi.org/10.1128/AEM.70.11.6686-6694.2004.

Møretrø, T., Schirmer, B.C.T., Heir, E., Fagerlund, A., Hjemli, P., Langsrud, S., 2017. Tolerance to quaternary ammonium compound disinfectants may enhance growth of Listeria monocytogenes in the food industry. Int. J. Food Microbiol. 241, 215–224. https://doi.org/10.1016/J.IJFOODMICRO.2016.10.025.

Moura, A., Criscuolo, A., Pouseele, H., Maury, M.M., Leclercq, A., Tarr, C., Bjorkman, J. T., Dallman, T., Reimer, A., Enouf, V., Larsonneur, E., Carleton, H., Bracq-Dieye, H., Katz, L.S., Jones, L., Touchon, M., Tourdjman, M., Walker, M., Stroika, S., Cantinelli, T., Chenal-Francisque, V., Kucerova, Z., Rocha, E.P., Nadon, C., Grant, K., Nielsen, E.M., Pot, B., Gerner-Smidt, P., Lecuit, M., Brisse, S., 2016. Whole genome-based population biology and epidemiological surveillance of Listeria monocytogenes. Nat. Microbiol. 2, 16185. https://doi.org/10.1038/nmicrobiol.2016.185.

Muyzer, G., De Waal, E.C., Uitterlinden, A.G., 1993. Profiling of complex microbial populations by denaturing gradient gel electrophoresis analysis of polymerase chain reaction-amplified genes coding for 16S rRNA. Appl. Environ. Microbiol. 59, 695. https://doi.org/10.1128/AEM.59.3.695-700.1993.

Nair, S., Frehel, C., Nguyen, L., Escuyer, V., Berche, P., 1999. ClpE, a novel member of the HSP100 family, is involved in cell division and virulence of Listeria monocytogenes. Mol. Microbiol. 31, 185–196. https://doi.org/10.1046/J.1365-2958.1999.01159.X.

Nightingale, K.K., Windham, K., Martin, K.E., Yeung, M., Wiedmann, M., 2005. Select Listeria monocytogenes subtypes commonly found in foods carry distinct nonsense mutations in inlA, leading to expression of truncated and secreted internalin A, and are associated with a reduced invasion phenotype for human intestinal. Appl. Environ. Microbiol. 71, 8764–8772. https://doi.org/10.1128/AEM.71.12.8764-8772.2005/ASSET/49570414-0517-41B3-9E26-FDB88B16B4C1/ASSETS/GRAPHIC/ZAM0120561390004.JPEG.

Nightingale, K.K., Ivy, R.A., Ho, A.J., Fortes, E.D., Njaa, B.L., Peters, R.M., Wiedmann, M., 2008. InlA premature stop codons are common among Listeria monocytogenes isolates from foods and yield virulence-attenuated strains that confer protection against fully virulent strains. Appl. Environ. Microbiol. https://doi.org/10.1128/AEM.00997-08.

Njage, P.M., Leekitcharoenphon, P., Hansen, L.T., Hendriksen, R.S., Faes, C., Aerts, M., Hald, T., 2020. Quantitative microbial risk assessment based on whole genome sequencing data: case of Listeria monocytogenes. Microorganisms. https://doi.org/10.3390/microorganisms8111772.

Olier, M., Pierre, F., Rousseaux, S., Lemaitre, J.P., Rousset, A., Piveteau, P., Guzzo, J., 2003. Expression of truncated internalin A is involved in impaired internalization of some Listeria monocytogenes isolates carried asymptomatically by humans. Infect. Immun. 71, 1217–1224. https://doi.org/10.1128/IAI.71.3.1217-1224.2003.

Olier, M., Garmyn, D., Rousseaux, S., Lemaître, J.P., Piveteau, P., Guzzo, J., 2005. Truncated internalin A and asymptomatic Listeria monocytogenes carriage: in vivo investigation by allelic exchange. Infect. Immun. 73, 644–648. https://doi.org/10.1128/IAI.73.1.644-648.2005/ASSET/25E1E5F9-13EF-402F-8572-98CBC814B4AE/ASSETS/GRAPHIC/ZII0010545160003.JPEG.

Painset, A., Björkman, J.T., Kiil, K., Guillier, L., Mariet, J.F., Felix, B., Amar, C., Rotariu, O., Roussel, S., Perez-Reche, F., Brisse, S., Moura, A., Lecuit, M., Forbes, K., Strachan, N., Grant, K., Møller-Nielsen, E., Dallman, T.J., 2019. Liseq – Whole-genome sequencing of a cross-sectional survey of Listeria monocytogenes in ready-to-eat foods and human clinical cases in Europe. Microb. Genomics. https://doi.org/10.1099/mgen.0.000257.

Paradis, E., Schliep, K., 2019. ape 5.0: an environment for modern phylogenetics and evolutionary analyses in R. Bioinformatics 35, 526–528. https://doi.org/10.1093/bioinformatics/bty633.

Popowska, M., Krawczyk-Balska, A., Ostrowski, R., Desvaux, M., 2017. InlL from Listeria monocytogenes is involved in biofilm formation and adhesion to mucin. Front. Microbiol. 8 https://doi.org/10.3389/FMICB.2017.00660.

Promadej, N., Fiedler, F., Cossart, P., Dramsi, S., Kathariou, S., 1999. Cell wall teichoic acid glycosylation in Listeria monocytogenes serotype 4b requires gtcA, a novel, serogroup-specific gene. J. Bacteriol. 181, 418–425. https://doi.org/10.1128/JB.181.2.418-425.1999.

Quereda, J.J., Nahori, M.A., Meza-Torres, J., Sachse, M., Titos-Jiménez, P., Gomez-Laguna, J., Dussurget, O., Cossart, P., Pizarro-Cerdá, J., 2017. Listeriolysin S is a streptolysin S-like virulence factor that targets exclusively prokaryotic cells in vivo. MBio. https://doi.org/10.1128/mBio.00259-17.

Quijada, N.M., Dzieciol, M., Schmitz-Esser, S., Wagner, M., Selberherr, E., 2022. Metatranscriptomic analyses unravel dynamic changes in the microbial and metabolic transcriptional profiles in artisanal Austrian hard-cheeses during ripening. Front. Microbiol. 483. https://doi.org/10.3389/FMICB.2022.813480.

R Core Team, 2020. European Environment Agency [WWW Document]. n.d. URL. https://www.eea.europa.eu/data-and-maps/indicators/oxygen-consuming-substances-in-rivers/r-development-core-team-2006 (accessed 3.14.22).

Ragon, M., Wirth, T., Hollandt, F., Lavenir, R., Lecuit, M., Le Monnier, A., Brisse, S., 2008. A new perspective on Listeria monocytogenes evolution. PLoS Pathog. 4, e1000146 https://doi.org/10.1371/journal.ppat.1000146.

Reis, O., Sousa, S., Camejo, A., Villiers, V., Gouin, E., Cossart, P., Cabanes, D., 2010. LapB, a novel Listeria monocytogenes LPXTG surface adhesin, required for entry into eukaryotic cells and virulence. J. Infect. Dis. 202, 551–562. https://doi.org/10.1086/654880.

Rousseaux, S., Olier, M., Lemaître, J.P., Piveteau, P., Guzzo, J., 2004. Use of PCR-restriction fragment length polymorphism of inlA for rapid screening of Listeria monocytogenes strains deficient in the ability to invade Caco-2 cells. Appl. Environ.

Microbiol. 70, 2180–2185. https://doi.org/10.1128/AEM.70.4.2180-2185.2004/ASSET/7AF28771-168A-44B8-AE07-B0BFC51ACD01/ASSETS/GRAPHIC/ZAM0040409890002.JPEG.

Rychli, K., Wagner, E.M.E.M., Ciolacu, L., Zaiser, A., Tasara, T., Wagner, M., Schmitz-Esser, S., 2017. Comparative genomics of human and non-human Listeria monocytogenes sequence type 121 strains. PLoS One 12, e0176857. https://doi.org/10.1371/journal.pone.0176857.

Sabet, C., Toledo-Arana, A., Personnic, N., Lecuit, M., Dubrac, S., Poupel, O., Gouin, E., Nahori, M.A., Cossart, P., Bierne, H., 2008. The Listeria monocytogenes virulence factor InlJ is specifically expressed in vivo and behaves as an adhesin. Infect. Immun. 76, 1368–1378. https://doi.org/10.1128/IAI.01519-07.

Schiavano, G.F., Ateba, C.N., Petruzzelli, A., Mele, V., Amagliani, G., Guidi, F., De Santi, M., Pomilio, F., Blasi, G., Gattuso, A., Di Lullo, S., Rocchegiani, E., Brandi, G., 2021. Whole-genome sequencing characterization of virulence profiles of Listeria monocytogenes food and human isolates and in vitro adhesion/invasion assessment. Microorganisms 10, 62. https://doi.org/10.3390/MICROORGANISMS10010062.

Schlech, W.F., 2019. Epidemiology and clinical manifestations of Listeria monocytogenes infection. Microbiol. Spectr. 7 https://doi.org/10.1128/MICROBIOLSPEC.GPP3-0014-2018.

Upham, J., Chen, S., Boutilier, E., Hodges, L., Eisebraun, M., Croxen, M.A., Fortuna, A., Mallo, G.V., Garduño, R.A., 2019. Potential ad hoc markers of persistence and virulence in Canadian Listeria monocytogenes food and clinical isolates. J. Food Prot. 82, 1909–1921. https://doi.org/10.4315/0362-028X.JFP-19-028.

Van Stelten, A., Simpson, J.M., Ward, T.J., Nightingale, K.K., 2010. Revelation by single-nucleotide polymorphism genotyping that mutations leading to a premature stop codon in inlA are common among Listeria monocytogenes isolates from ready-to-eat foods but not human listeriosis cases. Appl. Environ. Microbiol. 76, 2783–2790. https://doi.org/10.1128/AEM.02651-09.

Vázquez-Boland, J.A., Domínguez-Bernal, G., González-Zorn, B., Kreft, J., Goebel, W., 2001. Pathogenicity islands and virulence evolution in Listeria. Microbes Infect. 3, 571–584. https://doi.org/10.1016/S1286-4579(01)01413-7.

Wagner, E., Zaiser, A., Leitner, R., Quijada, N.M., Pracser, N., Pietzka, A., Ruppitsch, W., Schmitz-Esser, S., Wagner, M., Rychli, K., 2020. Virulence characterization and comparative genomics of Listeria monocytogenes sequence type 155 strains. BMC Genomics. https://doi.org/10.1186/s12864-020-07263-w.

Walle, I.Van, Björkman, J.T., Cormican, M., Dallman, T., Mossong, J., Moura, A., Pietzka, A., Ruppitsch, W., Takkinen, J., Mattheus, W., Christova, I., Maikanti-Charalampous, P., Karpíšková, R., Halbedel, S., Nielsen, E.M., Koolmeister, M., Mandilara, G., Torreblanca, R.A., Salmenlinna, S., Lecuit, M., Leclercq, A., Damjanova, I., Delappe, N., Sigmundsdóttir, G., Gattuso, A., Griškevičius, A., Ragimbeau, C., Franz, E., Brandal, L.T., Kuch, A., Borges, V., Caplan, D., Jernberg, C., Alm, E., Trkov, M., Tkacova, E., Grant, K., 2018. Retrospective validation of whole genome sequencingenhanced surveillance of listeriosis in Europe, 2010 to 2015. Eurosurveillance 23, 1–11. https://doi.org/10.2807/1560-7917.ES.2018.23.33.1700798/CITE/PLAINTEXT.

Wang, L., Lin, M., 2008. A novel cell wall-anchored peptidoglycan hydrolase (autolysin), IspC, essential for Listeria monocytogenes virulence: genetic and proteomic analysis. Microbiology. https://doi.org/10.1099/mic.0.2007/015172-0.

Wuenscher, M.D., Kohler, S., Bubert, A., Gerike, U., Goebel, W., 1993. The iap gene of Listeria monocytogenes is essential for cell viability, and its gene product, p60, has bacteriolytic activity. J. Bacteriol. 175, 3491–3501. https://doi.org/10.1128/JB.175.11.3491-3501.1993.